iScience

CellPress
OPEN ACCESS

Article

Global methane emissions from rice paddies: CH4MOD model development and application

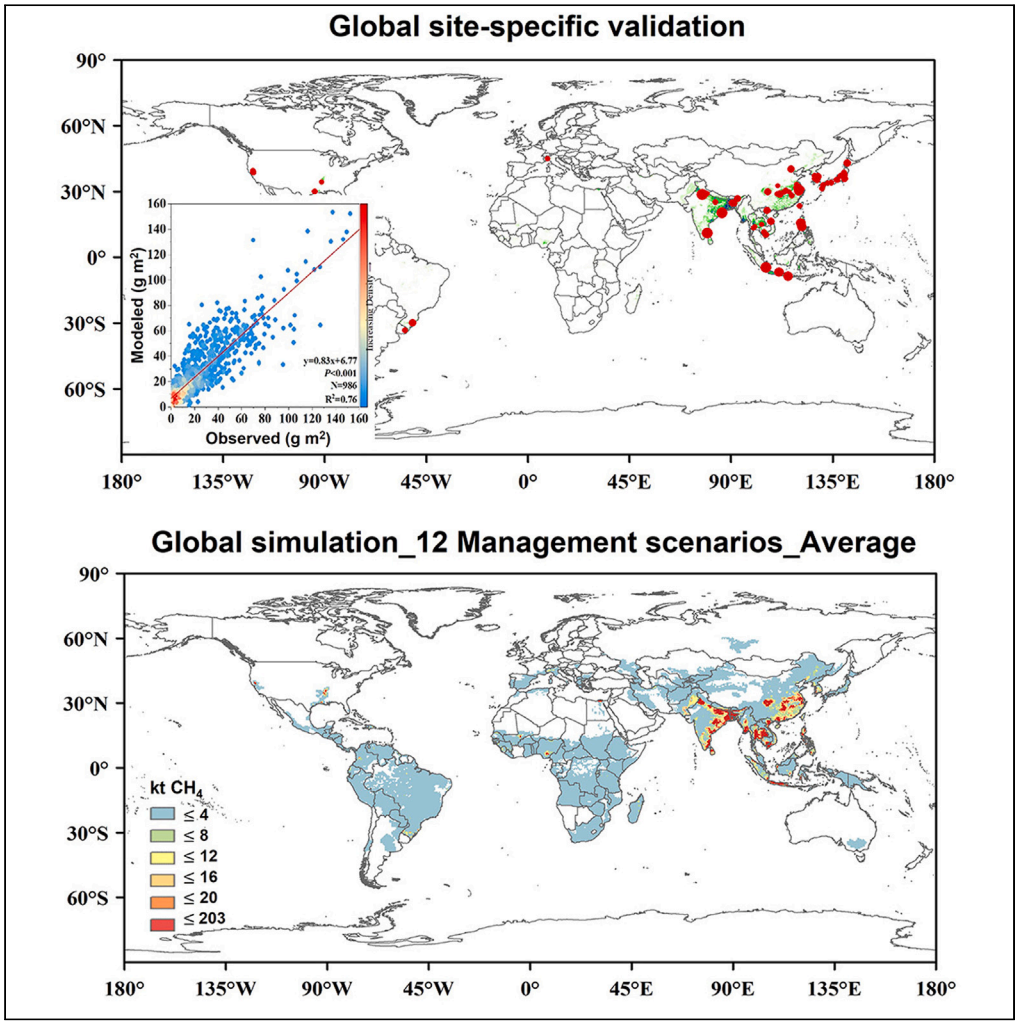

Qiwen Hu, Jingxian Li, Hanzhi Xie, ..., Xinqing Lu, Tingting Li, Zhangcai Qin

litingting@mail.iap.ac.cn

Highlights

CH4MOD model was globally validated and applied for estimating CH_4 emissions from rice

Water regime and organic matter amendment play major roles in CH_4 emission estimates

Global estimated CH_4 emissions varied largely with management scenarios

Hu et al., iScience 27, 111237
November 15, 2024
https://doi.org/10.1016/j.isci.2024.111237

iScience

CellPress
OPEN ACCESS

Article

Global methane emissions from rice paddies: CH4MOD model development and application

Qiwen Hu,[1,2,3,4] Jingxian Li,[1] Hanzhi Xie,[1] Yao Huang,[5,6] Josep G. Canadell,[7] Wenping Yuan,[3,4,8] Jinyang Wang,[9,10] Wen Zhang,[6] Lijun Yu,[6] Shihua Li,[1] Xinqing Lu,[1] Tingting Li,[2,3,4,11,*] and Zhangcai Qin[1,3,4]

SUMMARY

Rice cultivation constitutes a significant anthropogenic methane (CH_4) source and a crucial target for CH_4 mitigation. However, global and regional emissions remain poorly constrained. In this study, we validated a global-process-based methane model for rice paddies (CH4MOD), analyzed the sensitivity of major emission drivers, and simulated management scenarios involving four water regimes and three organic matter amendments. CH4MOD simulations achieved a correlation coefficient of 0.76 across 986 CH_4 flux observations globally, demonstrating its capability under different environmental conditions and management practices. The sensitivity analysis revealed water regime as the primary driver, followed by organic matter amendment and temperature. Under different crop management, CH_4 emissions varied significantly from 8 to 78 Tg CH_4/yr. This wide range of emissions demonstrates the need to use and improve rice-specific emission models and spatiotemporal data on rice distribution, water, and residue management for accurately assessing local to global emissions and their climate mitigation potential.

INTRODUCTION

Methane (CH_4) ranks second to carbon dioxide in contributing to global warming, accounting for 25% of the total impact.[1] Rapid reduction in CH_4 emissions could provide the most effective strategy to mitigate near-term global warming, according to the Global Methane Pledge signed at the 26th meeting of the Conference of the Parties of the UN Framework Convention on Climate Change.[2,3] Agriculture represents the leading anthropogenic CH_4 source, contributing 44% to the global anthropogenic CH_4 emissions,[4] and rice fields constitute the most important agricultural source.[5] Global CH_4 emissions originating from rice fields over the 2000–2009 period were revised from 36 (33–40) Tg CH_4/yr in the Fifth Assessment Report (AR5)[6] of the Intergovernmental Panel on Climate Change (IPCC) to 29 (25–37) Tg CH_4/yr in the AR6[7] document.[8]

CH_4 emissions originating from rice fields can be estimated using field measurements, emission factors, atmospheric inversions, data-driven methods, and process-based models.[9–11,34] Field measurement is a robust approach, but measurements are costly, time-consuming, and difficult to perform at large spatial scales.[12,13] Owing to its simplicity, the emission factor method recommended in IPCC Guidelines is widely used worldwide.[5,9,14] However, the accuracy is low given that emission factors generally represent mean values for large regions with divergent environmental conditions and management practices.[18] Atmospheric inversion methods for quantifying CH_4 emissions based on transport models and atmospheric CH_4 concentration observations[15] are attractive because they rely on observed atmospheric CH_4 concentrations to constrain estimates, but the limited availability of atmospheric observations, the poor performance of transport models in the tropics[16] as well as the uncertainties in prior inventories[17] restrict these estimates, especially for sector sources. Data-driven methods, such as machine learning and statistical models, can identify patterns and make predictions based on large datasets. These methods are particularly useful for regions with limited process-based model inputs or abundant empirical data.[18] However, they are also limited by the availability and frequency of data and lack the ability to provide mechanistic explanations.

[1]School of Atmospheric Sciences, Guangdong Province Data Center of Terrestrial and Marine Ecosystems Carbon Neutrality, Sun Yat-sen University, and Southern Marine Science and Engineering Guangdong Laboratory (Zhuhai), Zhuhai 519000, China
[2]Key Laboratory of Atmospheric Environment and Extreme Meteorology, Institute of Atmospheric Physics, Chinese Academy of Sciences, Beijing 100029, China
[3]International Research Center of Big Data for Sustainable Development Goals, Beijing 100094, China
[4]Southern Marine Science and Engineering Guangdong Laboratory (Zhuhai), Zhuhai 519000, China
[5]State Key Laboratory of Vegetation and Environmental Change, Institute of Botany, Chinese Academy of Sciences, Beijing 100093, China
[6]LAPC, Institute of Atmospheric Physics, Chinese Academy of Sciences, Beijing 100029, China
[7]Global Carbon Project, CSIRO Oceans and Atmosphere, Canberra, ACT 2601, Australia
[8]Institute of Carbon Neutrality, Sino-French Institute for Earth System Science, College of Urban and Environmental Sciences, Peking University, Beijing 100871, China
[9]Key Laboratory of Green and Low-carbon Agriculture in Southeastern China, Ministry of Agriculture and Rural Affairs, College of Resources and Environmental Sciences, Nanjing Agricultural University, Nanjing, China
[10]Jiangsu Key Laboratory of Low Carbon Agriculture and GHGs Mitigation, Jiangsu Collaborative Innovation Center for Solid Organic Waste Resource Utilization, Nanjing, China
[11]Lead contact
*Correspondence: litingting@mail.iap.ac.cn
https://doi.org/10.1016/j.isci.2024.111237

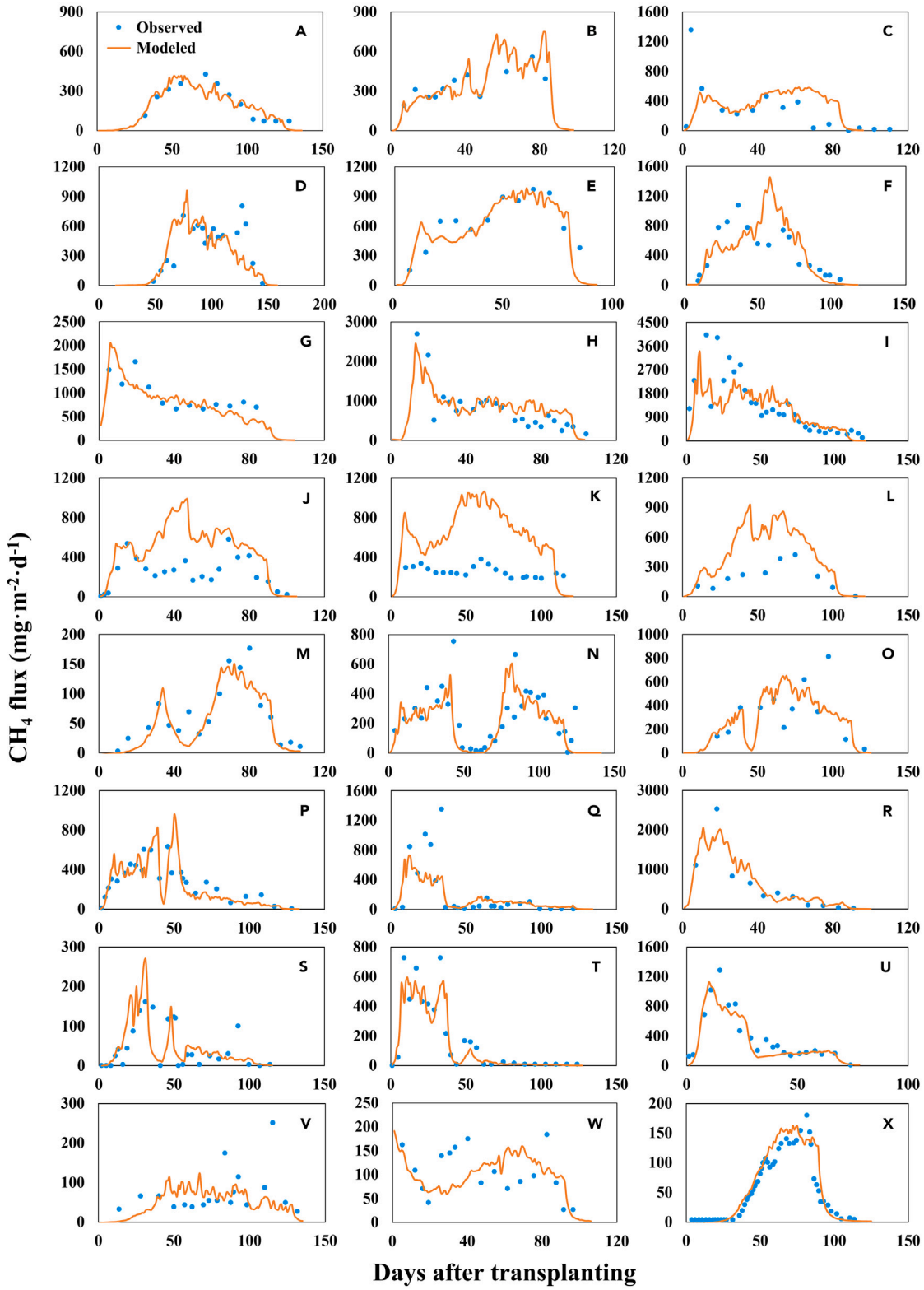

Figure 1. Comparison of the modeled and observed seasonal patterns of CH_4 emissions for single-rice cultivation

Water regime = F: (A) Bangladesh_2017,[74] (B) Vietnam_2013,[75] (C) India_2017–2018,[76] (D) Italy_2009,[77] (E) Indonesia_1994,[78] (F) Brazil_2002,[79] (G) Thailand_1992,[80] (H) USA_1992,[81] (I) South Korea_2008,[82] (J) India_1993,[83] (K) India_2011,[84] (L) India_1995[85]; water regime = FDF: (M) India_2017,[76] (N)

Figure 1. *Continued*
South Korea_2008,[86] (O) Japan_2010[25]; water regime = FDFM: (P) China_2014[87]; water regime = FM: (Q) China_2008,[88] (R) China_2011[89]; water regime = FDM: (S) China_2004,[90] (T) China_2006,[91] (U) Cambodia_2011[92]; water regime = M: (V) Japan_2003,[93] (W) India_2016[94]; water regime = RFW: (X) Indonesia_1995[95].

Most of the aforementioned approaches cannot fully account for the environmental and agricultural controls on rice paddy CH_4 emissions, such as temperature,[19] soil properties,[20,21] water management practice,[22–24] organic matter (OM) amendment,[25,74] and rice varieties,[26,27] or simulate potential CH_4 emissions under different climate conditions and management policies. Process-based models capture the mechanisms of CH_4 production, oxidation, and emission in rice paddies, incorporating the combined effects of the above controlling factors, which could be a promising approach for highly accurate regional-scale simulations. Furthermore, process-based models can consider climate factors and their evolution over time, rendering them the most comprehensive approach for assessing the potential for CH_4 mitigation in the rice sector. However, complete validation is an essential precondition for global application and mitigation prediction.

Current process-based models include the physical geochemical model DeNitrification-DeComposition (DNDC),[28] the ecosystem model DayCent,[29] the Dynamic Land Ecosystem Model (DLEM),[30] and the rice paddy CH_4 emission model CH4MOD.[13] Studies based on these models have focused on simulating CH_4 emissions originating from rice fields at regional scales, but limited validation may induce uncertainties when applied to global rice paddies with divergent agricultural management practices.[31–35] Moreover, non-continuous flooding and straw removal strategies are regarded as effective and low-cost mitigation strategies.[8,57] It is vital to evaluate the mitigation potential by adjusting combined management practices through a well-performing process-based model.

The CH4MOD model[13] exhibits the advantages of simple inputs and full consideration of primary human management. The model has been validated for CH_4 emissions originating from continuously flooded rice paddies across China, Italy, Indonesia, the Philippines, and the United States.[13] Furthermore, after incorporating a water regime module, this model has been comprehensively validated in China.[33] This study aimed to (1) incorporate different water management types and refine the parameterization of rice varieties in the CH4MOD model on a global scale and evaluate its performance in simulating CH_4 emissions stemming from rice fields in different agro-climatic zones with divergent management practices and (2) use it to conduct a scenario-based modeling experiment to estimate the impact of two primary controlling factors, e.g., the water regime and OM amendment. The goal was to better understand the significance and obtain insights for developing global strategies to mitigate CH_4 emissions stemming from rice paddies.

RESULTS

Global validation

Validation of the seasonal CH_4 variations

A comparison between the modeled and observed seasonal variations at single-rice cropping observations is shown in Figure 1. At the observations with continuous flooding (F), the CH4MOD model exhibited a unimodal pattern (Figures 1A–1L), in which the peaks were determined by the maximum biomass, highest temperature, and time of OM amendment. The peak corresponds to the plant growth peak without OM amendment (Figure 1A). OM amendment during the transplanting period advanced to the peak (Figures 1G–1I). The model also captured seasonal variations at the observations with different drainage practices (Figures 1M–1W), indicating its ability to describe the control of the water regime on CH_4 emissions. For example, it captured the bimodal patterns at FDF observations (Figures 1M and 1N). It also captured the low CH_4 emissions due to intermittent irrigation at the late growing stage (FDFM, Figure 1P; FM, Figures 1Q and 1R; FDM,

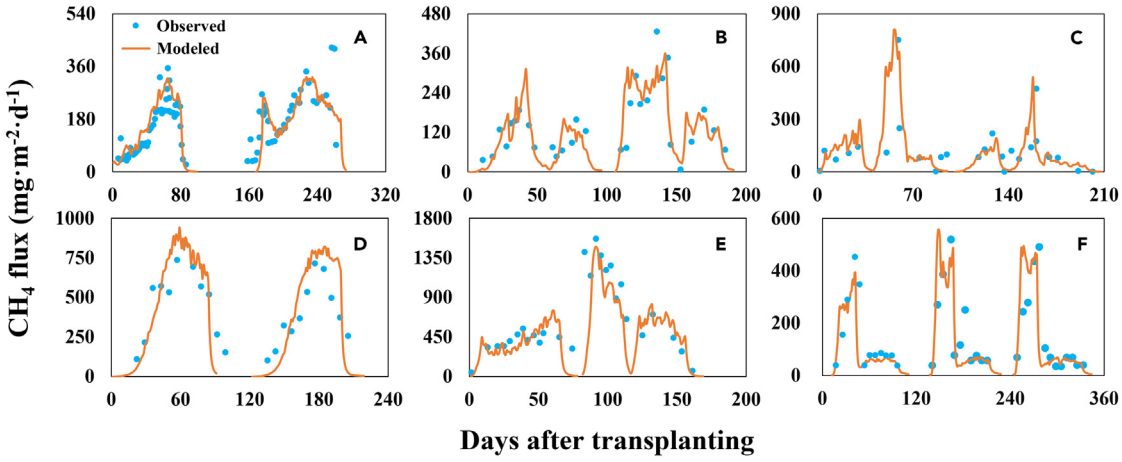

Figure 2. Comparison of the modeled and observed seasonal patterns of CH_4 fluxes for double-rice cultivation and triple-rice cultivation
Double-rice cultivation: (A) Philippines_1996,[96] (B)Vietnam_2017,[62] (C) China_2014,[97] (D) Indonesia_1995,[98] (E) China_2007.[99] Triple-rice cultivation: (F) Vietnam_2015.[100]

Figures 1S–1U) and during the whole growing season (M, Figures 1V and 1W). Overall, the CH4MOD model could generally capture the seasonal patterns of CH_4 emissions under different climatic conditions and soil environments with varying agricultural management practices under single-rice cultivation, except for some overestimation at Indian sites (Figures 1J–1I).

Figure 2 shows a comparison of the modeled and observed seasonal variations for double-/triple-cropped rice. With a gap of 1 to 2 months between the two seasons, double-cropped rice exhibited more similar behavior to that observed for two independent single-cropped rice seasons. Flooding and drainage controlled the peaks and minimum values, respectively. The model accurately simulated two peaks corresponding to rice maturity at continuous flooding observations (Figures 2A and 2D). The model also performed well in capturing the four peaks (Figures 2B and 2C) and three peaks (Figure 2E) due to mid-season drainage. Rice residue of the first season may enhance the peak value of the second season, e.g., Figures 2B and 2E, which the model could capture well. In Figure 2C, the first-season peak is higher because no OM is added during the second season. Overall, the CH4MOD model performed well in simulating the seasonal CH_4 variations in both double- and triple-rice fields.

Validation of the seasonal total CH_4 emissions

Globally, the observed seasonal emissions ranged from 1.01 to 177.18 g m^{-2}, with an average value of 23.32 g m^{-2}. Consistent with the observations, the model simulations yielded an average value of 25.4 g m^{-2}, with a range from 1.58 to 155.16 g m^{-2}. The regression of the modeled values against the observed seasonal total emissions (Figure 3A) yielded an R^2 value of 0.78, with a slope of 0.85 and an intercept of 5.57 (n = 986, $p < 0.001$). The RMSE, MAE, and EF values were 11.64, 7.85, and 0.78, respectively (Table 1). The EF value indicated that the model performs excellently globally.

Regression analysis indicated that the model performed well in simulating the total seasonal CH_4 emissions at observations inside (Figure 3B) and outside Asia (Figure 3C). The correlation coefficients were 0.77 and 0.76, respectively, with slopes of 0.81 and 0.97, respectively (Figures 3B and 3C, respectively). The statistical analysis results revealed better model performance at Asian observations than outside Asia, with lower RMSE and MAE and higher EF values (Table 1). Among the Asian observations, the model performance was good in China and India (EF = 0.71 and 0.63, respectively) and excellent in the other Asian countries (Table 1). The Chinese locations exhibited a correlation coefficient of 0.72 and a slope of 0.77 (Figure 3D). In India, the regression of the modeled values against the observed seasonal total emissions (Figure 3E) yielded an R^2 value of 0.68, with a slope of 0.93 and an intercept of 3.77 (n = 192, $p < 0.001$). Moreover, the regression was

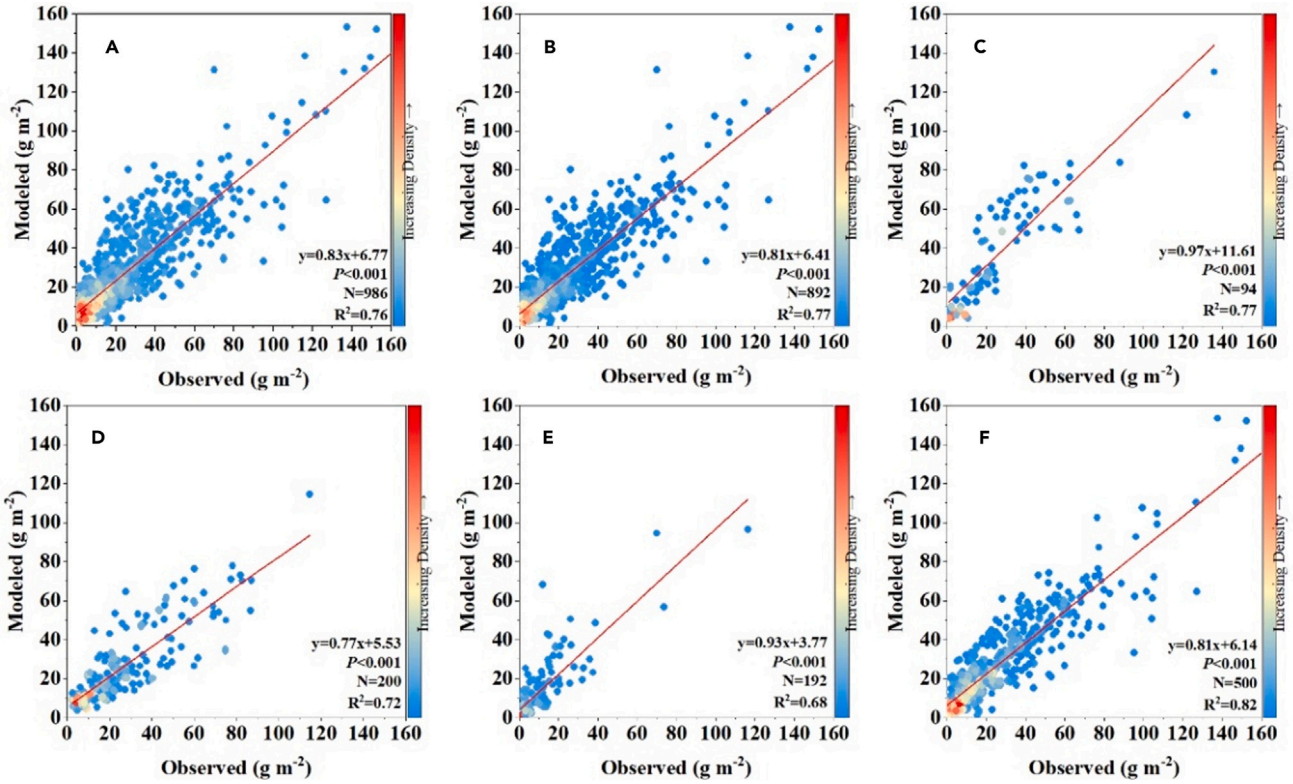

Figure 3. Comparison of the observed and modeled seasonal total CH_4 fluxes

(A) Global, (B) Asia, (C) continents other than Asia, (D) China, (E) India, (F) other Asian countries except China and India. The red solid lines are the regression lines indicating the relationship between observed and modeled seasonal total CH_4 fluxes. The F-test was used to test whether the regression model was statistically significant overall. N is the total number of observations in the region.

Table 1. Model performance with site observations in different regions

	Global	Asia	Other[a]	China	India	Other Asia[b]
RMSE	11.64	10.80	17.76	11.29	8.99	11.23
MAE	7.85	7.26	13.42	8.10	5.63	7.55
R^2	0.76	0.77	0.76	0.72	0.68	0.82
EF	0.78	0.81	0.52	0.71	0.63	0.82

RMSE, Root-mean-square error; MAE, Mean absolute error; R^2, Model coefficient of determination; EF, Model efficiency.
[a]Other continents except Asia.
[b]Other Asian countries except China and India.

characterized by the lowest RMSE and MAE values, at 8.99 and 5.63, respectively (Table 1). The highest R^2 and EF values of the simulations, at 0.82, were observed in the other Asian countries (Table 1).

Sensitivity analysis

Human activities significantly influence CH_4 emissions from rice paddies. CH_4 flux was most sensitive to irrigation practices (IRRI), followed by organic matter input (OM). Globally, CF led to a 56% increase in CH_4 emissions, whereas FDF resulted in a 25% increase in emissions (Figure 4A). Conversely, multiple drainages could reduce CH_4 emissions by 30% under FDFM, followed by FM (37%), FDM, and M (approximately 60%). At the Chinese sites, due to the more commonly used water regimes, such as FDFM and FDM, CF and FDF resulted in higher CH_4 variations, increasing by 76% and 48%, respectively, whereas FDFM decreased CH_4 emissions by only 7% (Figure 4B). In India, where multiple intermittent drying events are common, CF led to a significant increase in emissions of up to 114% (Figure 4C). Regarding OM input, an increase of 50 g/m^2 (equivalent to a 9% increase in straw retention at the current global average yield of 460 g/m^2) corresponded to a 16% increase in CH_4 emissions originating from rice fields. Increases of 100 and 200 g/m^2 in *OM* led to CH_4 emission increases of 29% and 55%, respectively (Figure 4A). The lower impact of *OM* reduction could be attributed to the convention of treating negative *OM* values as zero. The impact of *OM* percentage changes in China was greater than that in India due to the higher baseline. When *OM* was increased

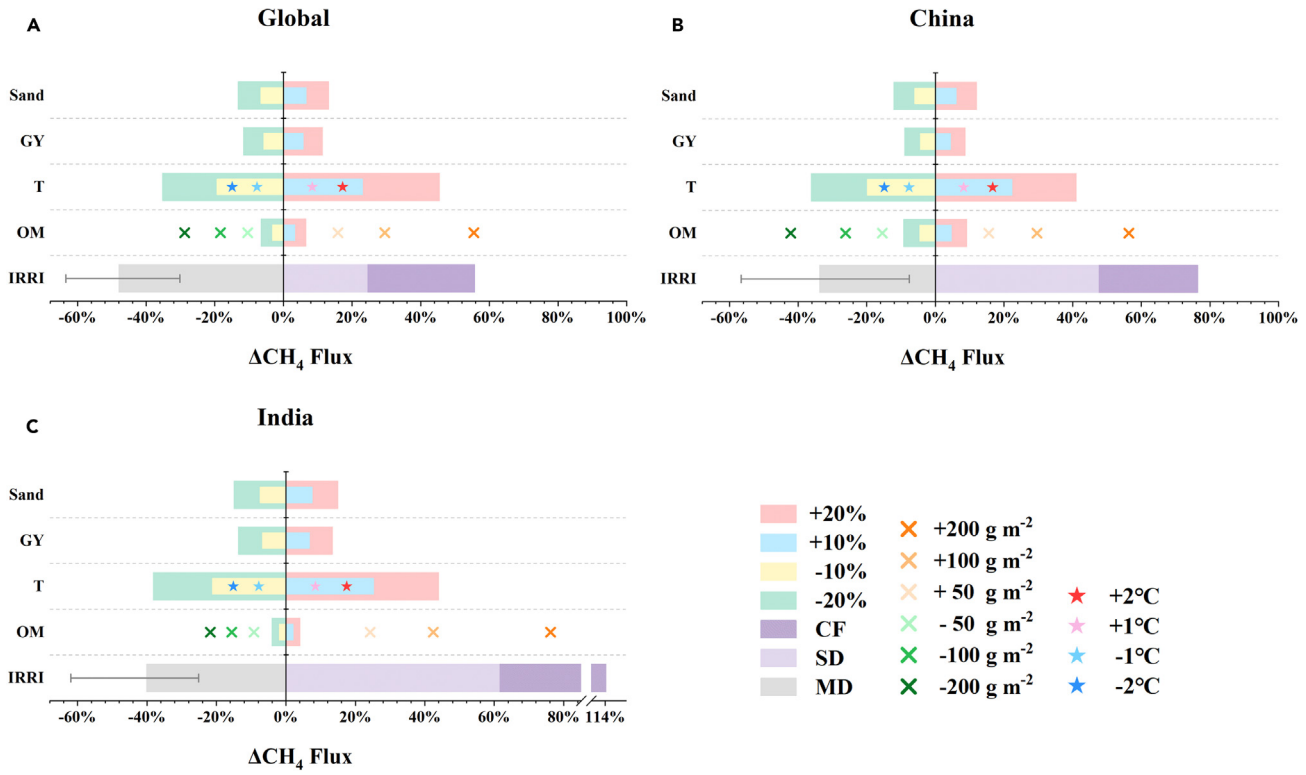

Figure 4. Sensitivity of the CH_4 emissions to the model inputs

(A) Global, (B) China, (C) India. For MD, the average values of FDFM, FDM, FM, and M are considered, with the gray bars denoting the maximum and minimum values.

by 20%, the CH_4 emissions increased by 9% (Figure 4B). In contrast, there was less *OM* amendment in India, and a 20% increase in *OM* resulted in only a 4% increase in CH_4 emissions.

Environmental factors, such as temperature and soil properties, also play a crucial role in determining CH_4 emissions from rice fields. An increase of 10% or 20% in *T* could result in the CH_4 fluxes increasing by 23% and 45%, respectively, with a slightly lower sensitivity to a decrease in T. Within the actual range of *T* variation, a fluctuation of 2°C corresponded to a CH_4 emission change of 16% (Figure 4A). In addition, a 20% change in the global *SAND* and *GY* values led to CH_4 emission variations of 13% and 11%, respectively. However, the higher baseline of *SAND* in India caused higher sensitivity (Figure 4C).

Scenario-based global rice CH_4 emissions

The global simulations indicated that the annual mean global rice CH_4 emissions varied between 8 and 78 Tg CH_4/yr under the 12 scenarios, with an average of 45 Tg CH_4/yr (Figure 5A). Spatially, Asian countries, including China (9.10 Tg CH_4/yr), India (11.84 Tg CH_4/yr), Thailand (3.69 Tg CH_4/yr), Bangladesh (3.2 Tg CH_4/yr), Vietnam (2.6 Tg CH_4/yr), and Indonesia (3.11 Tg CH_4/yr), collectively contributed 74.57% to the global emissions (Figure 5B). The emission hotspots were predominantly located in southeastern China, the Indian Ganges Plain and southeastern areas, southern Myanmar, Bangladesh, Thailand, and Java Island (Indonesia).

The wide range indicated that the global CH_4 emissions highly depended on the OM amendments and water regimes, but emission hotspots are still primarily determined by cultivation area. The three highest global emissions resulted from RF50_CF (78 Tg CH_4/yr), RF50_SD (70 Tg CH_4/yr), and RF30_CF (69 Tg CH_4/yr). RF0 combined with RATIO, SD, and MD resulted in the lowest global emissions, at 22, 21, and 8 Tg CH_4/yr, respectively. Under the same straw retention rate, CH_4 emissions were highest under the CF regime and 2.2–5 times lower under the MD regime. Globally, the average CV between the scenarios was 46%, ranging from 31% to 72% (Figure 5C). The greatest range occurred in Japan (61%), followed by China (53%), Bangladesh (53%), and India (49%).

The spatial distributions of the differences in CH_4 emissions normalized by the average values among the 12 scenarios are shown in Figures 6 and 7. The differences varied with respect to straw retention fraction changes (Figure 6). The difference between RF0 and RF30 was disproportionately greater than that between RF50 and RF30 under the same water regimes, even exceeding a factor of two. On a global

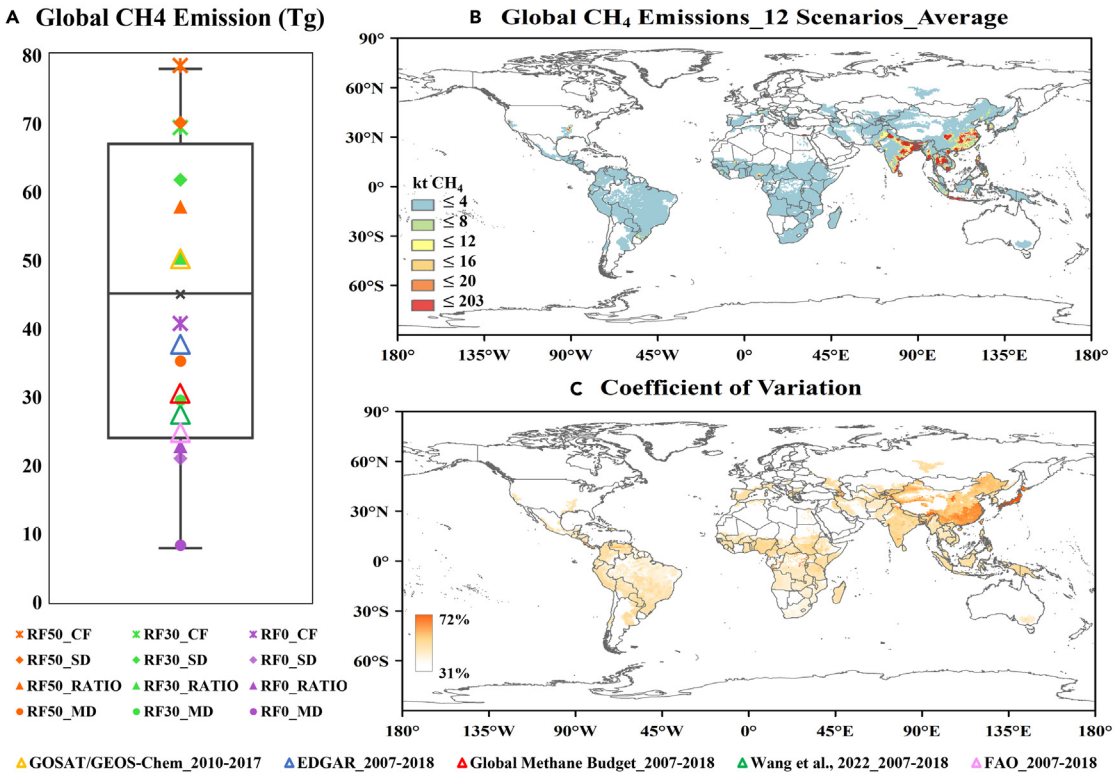

Figure 5. Scenario-based global rice CH_4 emissions simulations

(A) Boxplots comparing the global total CH_4 emissions for the 12 scenarios and comparison with other studies. The five solid lines of the boxplot correspond to the maximum, upper quartile, median, lower quartile, and minimum (from top to bottom).

(B) Spatial distribution of the annual mean CH_4 emissions from 2008 to 2017 for the average of the 12 scenarios.

(C) Spatial distribution of the coefficient of variations, which was introduced to evaluate the discrepancies between different scenarios.

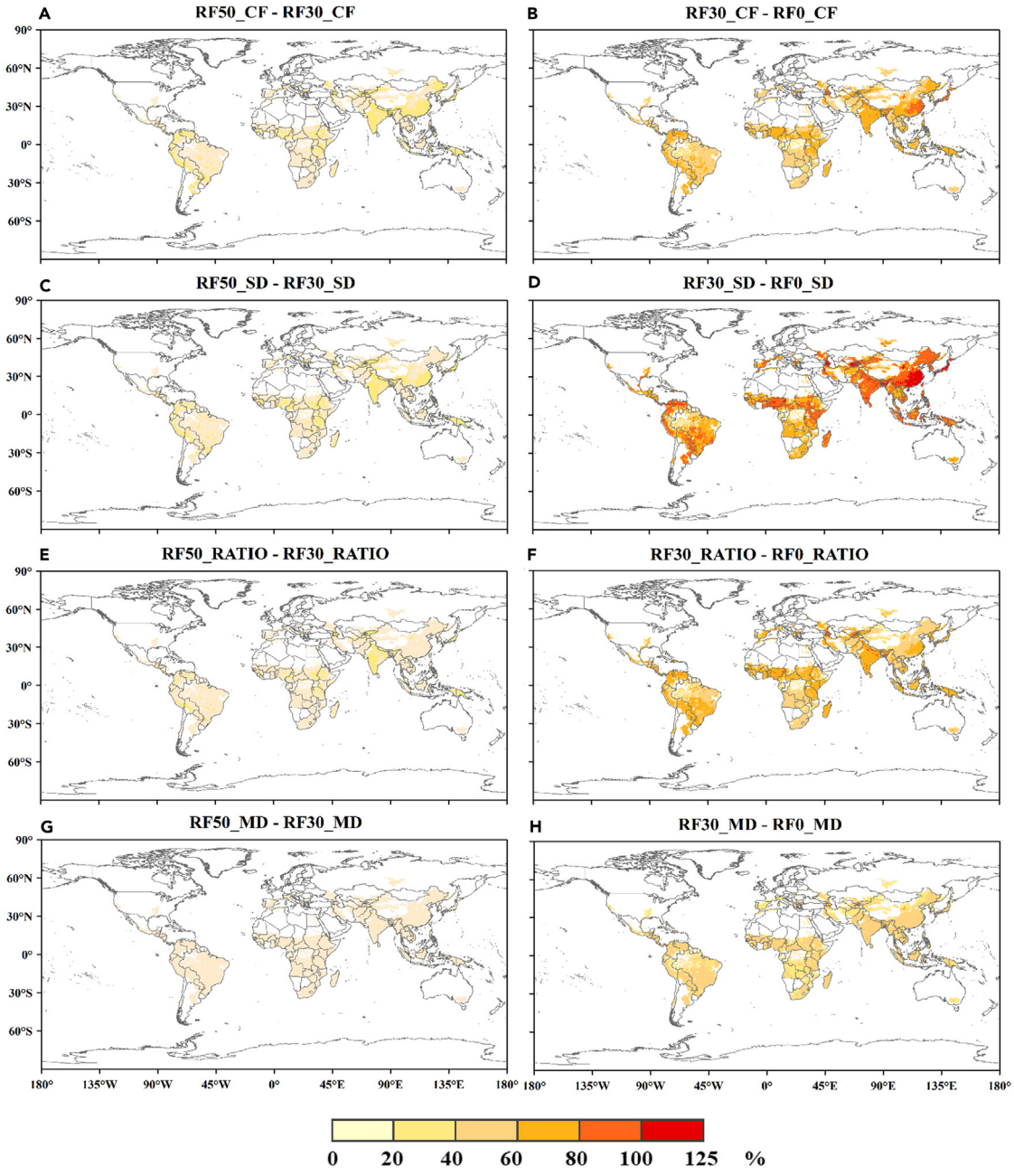

Figure 6. Spatial distribution of the differences in the global rice field CH_4 emissions under varying straw retention rates with the same water regime

The differences are normalized by the average of the 12 scenarios.

scale, the CH_4 emissions decreased by 57%, 74%, 56%, and 40% when RF30 was changed to RF0 under CF (Figure 6B), SD (Figure 6D), RATIO (Figure 6F), and MD (Figure 6H), respectively. When RF50 was changed to RF30, the CH_4 emissions decreased by only 18%, 18%, 16%, and 12% under CF (Figure 6A), SD (Figure 6C), RATIO (Figure 6E), and MD (Figure 6G), respectively. On a global scale, the differences in China and India were slightly greater than those in the other regions, especially between RF30_SD and RF0_SD, with a difference of approximately 88%.

The differences also varied between water regime changes under the same straw retention conditions (Figure 7). The CH_4 emissions decreased by changing CF to SD, with a maximum reduction of 42% under RF0 (Figure 7A), followed by 25% under RF30 (Figure 7B) and RF50 (Figure 7C). The differences between SD and RATIO exhibited varying spatial distributions globally (Figures 7D–7F). The CH_4 emissions under the RF0_SD scenario were higher than those under the RF0_RATIO scenario in China, Bangladesh, and northern Japan, but the opposite was true in the other regions (Figure 7D). However, when exogenous OM was added, SD resulted in higher emissions than RATIO globally,

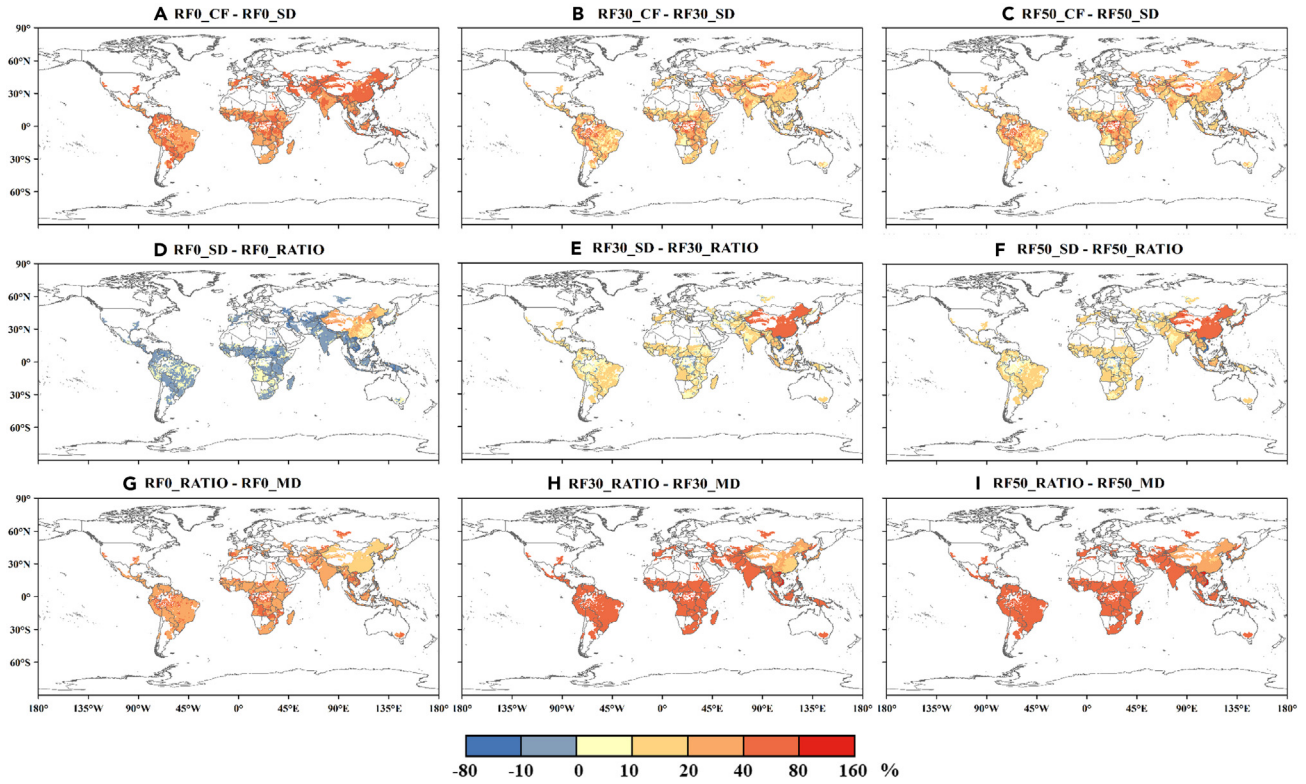

Figure 7. Spatial distribution of the differences in the global rice field CH_4 emissions under varying water regimes with the same straw retention rates

The differences are normalized by the average of the 12 scenarios.

except in Vietnam (Figures 7E and 7F). This was primarily due to Vietnam encompassing all flooding conditions under RATIO, whereas China, Japan, and Bangladesh now mainly employed MD. Therefore, the difference between RATIO and MD was smaller in China, Japan, and Bangladesh but larger in Vietnam (Figures 7G–7I). Under RF0, the average relative difference between RATIO and MD was 35% (Figure 7G), whereas under RF30 and RF50, it was 50% and 54%, respectively (Figures 7H and 7I).

DISCUSSION

The global simulations in this study indicated that the annual mean global rice CH_4 emissions vary between 8 and 78 Tg CH_4/yr under the 12 management scenarios, with an average of 45 Tg CH_4/yr (Figure 5A). The use of different input data within the same simulation method resulted in variations in methane emissions across management scenarios, underscoring the importance of the water regime and organic fertilizer application for global CH_4 emissions in rice paddies. The results also revealed the emission reduction potential of the different management approaches. Non-continuous flooding and straw removal strategies are effective mitigation strategies, as previously reported.[8,36,57] Current research on these mitigation strategies focuses on a single measure[53,59] or is conducted at the site or small regional scale.[37,60] Our simulations showed that the emission reduction effectiveness varies among the different management combinations and regions (Figures 6 and 7), demonstrating the necessity of comprehensive estimates by considering combined strategies at the national or global scale. Recent reduction strategies have also included improving rice varieties[38,39] and applying biochar.[40] However, these strategies necessitate improved quantifications and reduced costs.[41–43]

Moreover, emission reduction must be considered comprehensively, accounting for food security, ecological sustainability, and regional characteristics. Under the MD scenario, the CH_4 emissions were the lowest, demonstrating the greatest potential for emission reduction through changes in the water regime. However, MD requires comprehensive consideration of the optimal timing and duration of mid-season drainage to maintain rice production. Previous studies have suggested that straw removal can reduce CH_4 emissions, which is consistent with our simulations (Figure 6). However, this approach may hinder the increase in soil fertility and rice yield.[60,61] Future research should comprehensively consider soil organic carbon, rice yield, and CH_4 emissions to determine the optimal balance for food security and climate mitigation.

Current global estimates of CH_4 emissions stemming from rice paddies are mainly based on ground and satellite inversion methods. These include GOAST inversion estimate of 43 Tg CH_4/yr (2010–2017),[44] the Tier 1 method of the IPCC guidelines, e.g., EDGAR estimate of 37 Tg CH_4/yr (2007–2018),[45] FAO estimate of 24 Tg CH_4/yr (2007–2018),[46] Global Methane Budget (2007–2018) estimate of 30 Tg CH_4/yr,[4] and

statistical model estimate of 27 Tg CH_4/yr (2007–2018),[8] and the results fall within the range of the 12 scenarios analyzed in this study (Figure 5A). The process-based model approach of our study provides the unique capacity to attribute fluxes to actual driving processes, including climate change and management, while allowing us to estimate the potential for emission reduction. However, sufficient validations under different climate and soil conditions as well as management practices are indispensable for regional and global applications. Process-based models that can simulate CH_4 emissions stemming from rice paddies include DNDC,[28] DLEM,[30] and CH4MOD. DNDC and DLEM are comprehensive biogeochemical models, which describe carbon and nitrogen dynamics in croplands and focus on CO_2, CH_4, and N_2O greenhouse gases emissions. Therefore, the complicated processes require more inputs and complex parameterizations when extrapolating to a large scale. For example, ammonium, nitrate, urea, and anhydrous ammonia and their depth of application are needed as the inputs in the DNDC model,[28] which are hard to obtain on a global scale. The CH4MOD model, with its simplified processes, only focuses on CH_4 emissions, requiring fewer parameters, which is advantageous for both site-specific validation and CH_4 estimation on a global scale.[33] In this study, a large and comprehensive database of observations encompassing all major areas of rice paddies in the world was compiled, and global validation of the CH4MOD model was performed. The results indicated its effectiveness in simulating CH_4 emissions in rice paddies under various climate, soil, and agricultural management conditions.

Although our process-based model approach offers unique insights into the driving mechanisms of CH_4 emissions, acknowledging and addressing these uncertainties is essential for improving the accuracy and applicability of global rice field CH_4 emission estimates. Some other aspects can be improved for both modeling and global application. Regarding CH4MOD model, one of the advantages is its simplified processes and fewer required parameters, but this also introduces some limitations. It simplifies the rice growth process with yield data as input and does not simulate net primary productivity (NPP), which can introduce uncertainties if future yield data are unavailable or unreliable. For example, field experiments show significant impacts of rice varieties and rainfed conditions on methane emissions.[47,48] However, due to the diversity of rice varieties and complex rainfall patterns, the model currently uses default values for parameters related to rice varieties (such as *VI* and *r*) and *Eh* under rainfed conditions. More experimental data are needed to compare the methane emission potential of different rice varieties and dynamically measure *Eh* under rainfall conditions. Additionally, nitrogen fertilization affects the activity of methanogens and methanotrophs, soil organic matter, and redox potential.[49] The impact of nitrogen fertilization on methane emissions remains controversial due to varying soil conditions, microbial community responses, and environmental factors.[50] The amount, timing, and type of nitrogen fertilizer all significantly influence methane emissions.[51–53] Given these complexities and the current lack of specific nitrogen fertilizer data, CH4MOD does not currently account for nitrogen fertilizer effects but could be improved in the future.

To assess "real-world" rather than scenario-based CH_4 emissions, the areal change and global spatial distribution of rice, agricultural management, and region-specific validation should be explicitly examined. Significant changes, such as the rapid expansion of rice areas in some African countries[54] and changes in the spatial pattern of rice planting areas in China,[55] could affect regional simulation. Changes in crop rotation practices,[56] water management methods,[57–59] and straw incorporation rates[60,61] can also significantly impact methane emissions. For instance, over the past few decades, multiple cropping has developed rapidly in China, but since the year 2000, the increase of cash crops led to reduced rice rotation intensity, e.g., from triple- to double-cropping or from double- to single-cropping in some areas.[55] Globally, there is a growing emphasis on water-saving irrigation and maximizing straw utilization.[25,62] However, these practices are often not well documented, adding to the uncertainty of global and regional estimation. Moreover, high-quality observational data from regions like Africa and India are particularly limited but desired. More robust data collection efforts in these regions are necessary to improve regional modeling feasibility.

Limitations of this study

Despite great efforts for global model validation, there is still room for further improvement in terms of mechanistic understanding (e.g., carbon-nitrogen dynamics), regional representativeness (e.g., emerging rice in Africa), and global validation. For real-world estimation of global methane emissions, large data gaps should be filled to replace the scenario-based assessment regarding worldwide management practice. In particular, global spatially explicit data should be further acquired, including crop rotation, crop yield, rice area change and spatial distribution, water management by time and location (or at least region), and organic matter amendment by type and amount. Future collaborations in both data and modeling could be beneficial for understanding rice methane emissions and potential reduction.

RESOURCE AVAILABILITY

Lead contact

Further information and requests should be directed to and will be fulfilled by the lead contact, Prof. Tingting Li (*litingting@mail.iap.ac.cn*).

Materials availability

This study did not generate new unique materials.

Data and code availability

- This paper analyzes existing, publicly available data. These accession numbers for the datasets are listed in the key resources table.
- This paper does not report the original code.
- Any additional information required to reanalyze the data reported in this paper is available from the lead contact upon request.

ACKNOWLEDGMENTS

This work was funded by the Open Research Program of the International Research Center of Big Data for Sustainable Development Goals (CBAS2023ORP02), the National Natural Science Foundation of China (41975113), and the China Scholarship Council. The project was designed as a contribution to the Global Methane Budget of the Global Carbon Project and "Earth System Science Numerical Simulator Facility" (EarthLab).

AUTHOR CONTRIBUTIONS

Conceptualization and methodology, T.L., Z.Q., and Y.H.; formal analysis, Q.H., J.L., H.X., T.L., Z.Q.; resources, Y.H., J.C., W.Y., W.Z.; data curation, Q.H., J.W., L.Y., S.L., X.L.; writing—original draft, Q.H., T.L., Z.Q.; writing—review & editing, all; supervision, Z.Q. and T.L.; project administration: T.L. and Z.Q.

DECLARATION OF INTERESTS

The authors declare no competing interest.

STAR★METHODS

Detailed methods are provided in the online version of this paper and include the following:

SUPPLEMENTAL INFORMATION

Supplemental information can be found online at https://doi.org/10.1016/j.isci.2024.111237.

Received: February 27, 2024
Revised: June 27, 2024
Accepted: October 21, 2024
Published: October 23, 2024

REFERENCES

1. IPCC (2021). In Climate Change 2021: The Physical Science Basis. Contribution of Working Group I to the Sixth Assessment Report of the Intergovernmental Panel on Climate Change, V. Masson-Delmotte, P. Zhai, A. Pirani, S.L. Connors, C. Péan, S. Berger, N. Caud, Y. Chen, L. Goldfarb, and M.I. Gomis, eds. (Cambridge, United Kingdom and New York, NY, USA: Cambridge University Press), p. 2391. https://doi.org/10.1017/9781009157896.
2. Nisbet, E.G., Manning, M.R., Dlugokencky, E.J., Fisher, R.E., Lowry, D., Michel, S.E., Myhre, C.L., Platt, S.M., Allen, G., Bousquet, P., et al. (2019). Very strong atmospheric methane growth in the 4 years 2014–2017: Implications for the Paris Agreement. Global Biogeochem. Cycles *33*, 318–342. https://doi.org/10.1029/2018GB006009.
3. Kuylenstierna, J.C., Michalopoulou, E., and Malley, C. (2021). Global Methane Assessment: Benefits and Costs of Mitigating Methane Emissions (Sweden: Stockholm Environment Institute). https://policycommons.net/artifacts/1528411/global-methane-assessment/2218096.
4. Saunois, M., Stavert, A.R., Poulter, B., Bousquet, P., Canadell, J.G., Jackson, R.B., Raymond, P.A., Dlugokencky, E.J., Houweling, S., Patra, P.K., et al. (2020). The global methane budget 2000–2017. Earth Syst. Sci. Data *12*, 1561–1623. https://doi.org/10.5194/essd-12-1561-2020.
5. Carlson, K.M., Gerber, J.S., Mueller, N.D., Herrero, M., MacDonald, G.K., Brauman, K.A., Havlik, P., O'Connell, C.S., Johnson, J.A., Saatchi, S., et al. (2017). Greenhouse gas emissions intensity of global croplands. Nat. Clim. Change *7*, 63–68. https://doi.org/10.1038/nclimate3158.
6. Canadell, J.G., Monteiro, P.M., Costa, M.H., Da Cunha, L.C., Cox, P.M., Eliseev, A.V., and Lebehot, A.D. (2021). Global Carbon and Other Biogeochemical Cycles and Feedbacks (Cambridge University Press), pp. 673–816. https://www.ipcc.ch/report/ar6/wg1/chapter/chapter-5/.
7. Ciais, P., Sabine, C., Bala, G., Bopp, L., Brovkin, V., Canadell, J., and Thornton, P. (2013). Carbon and other biogeochemical cycles. Climate change 2013: the physical science basis. Contribution of Working Group I to the Fifth Assessment Report of the Intergovernmental Panel on Climate Change. Comput. Geom. *18*, 95–123. https://www.ipcc.ch/report/ar5/syr/.
8. Wang, J., Ciais, P., Smith, P., Yan, X., Kuzyakov, Y., Liu, S., Li, T., Zou, J., and Zou, J. (2023). The role of rice cultivation in changes in atmospheric methane concentration and the Global Methane Pledge. Global Change Biol. *29*, 2776–2789. https://doi.org/10.1111/gcb.16631.
9. Crippa, M., Solazzo, E., Guizzardi, D., Monforti-Ferrario, F., Tubiello, F.N., and Leip, A. (2021). Food systems are responsible for a third of global anthropogenic GHG emissions. Nat. Food *2*, 198–209. https://doi.org/10.1038/s43016-021-00225-9.
10. Wang, J., Akiyama, H., Yagi, K., and Yan, X. (2018). Controlling variables and emission factors of methane from global rice fields. Atmos. Chem. Phys. *18*, 10419–10431. https://doi.org/10.5194/acp-18-10419-2018.
11. Zhang, W., Yu, Y., Huang, Y., Li, T., and Wang, P. (2011). Modeling methane emissions from irrigated rice cultivation in China from 1960 to 2050. Global Change Biol. *17*, 3511–3523. https://doi.org/10.1111/j.1365-2486.2011.02495.x.
12. Malyan, S.K., Bhatia, A., Kumar, A., Gupta, D.K., Singh, R., Kumar, S.S., Tomer, R., Kumar, O., Jain, N., and Jain, N. (2016). Methane production, oxidation and mitigation: A mechanistic understanding and comprehensive evaluation of influencing factors. Sci. Total Environ. *572*, 874–896. https://doi.org/10.1016/j.scitotenv.2016.07.182.
13. Huang, Y., Sass, R.L., and Fisher, J.,F.M. (1998). A semi-empirical model of methane emission from flooded rice paddy soils. Global Change Biol. *4*, 247–268. https://doi.org/10.1046/j.1365-2486.1998.00129.x.
14. Yan, X., Akiyama, H., Yagi, K., and Akimoto, H. (2009). Global estimations of the inventory and mitigation potential of

methane emissions from rice cultivation conducted using the 2006 Intergovernmental Panel on Climate Change Guidelines. Global Biogeochem. Cycles *23*. https://doi.org/10.1029/2008GB003299.

15. Thompson, R.L., Stohl, A., Zhou, L.X., Dlugokencky, E., Fukuyama, Y., Tohjima, Y., Kim, S., Lee, H., Nisbet, E.G., Fisher, R.E., et al. (2015). Methane emissions in East Asia for 2000–2011 estimated using an atmospheric Bayesian inversion. JGR. Atmospheres *120*, 4352–4369. https://doi.org/10.1002/2014JD022394.
16. Cusworth, D.H., Bloom, A.A., Ma, S., Miller, C.E., Bowman, K., Yin, Y., Maasakkers, J.D., Zhang, Y., Scarpelli, T.R., Qu, Z., et al. (2021). A Bayesian framework for deriving sector-based methane emissions from top-down fluxes. Commun. Earth Environ. *2*, 242. https://doi.org/10.1038/s43247-021-00312-6.
17. Shen, L., Jacob, D.J., Gautam, R., Omara, M., Scarpelli, T.R., Lorente, A., Zavala-Araiza, D., Lu, X., Chen, Z., Lin, J., and Lin, J. (2023). National quantifications of methane emissions from fuel exploitation using high resolution inversions of satellite observations. Nat. Commun. *14*, 4948. https://doi.org/10.1038/s41467-023-40671-6.
18. Sun, J., Wang, M., Xu, X., Cheng, K., Yue, Q., and Pan, G. (2020). Re-estimating methane emissions from Chinese paddy fields based on a regional empirical model and high-spatial-resolution data. Environ. Pollut. *265*, 115017. https://doi.org/10.1016/j.envpol.2020.115017.
19. Qian, H., Zhang, N., Chen, J., Chen, C., Hungate, B.A., Ruan, J., Huang, S., Cheng, K., Song, Z., Hou, P., et al. (2022). Unexpected parabolic temperature dependency of CH4 emissions from rice paddies. Environ. Sci. Technol. *56*, 4871–4881. https://doi.org/10.1021/acs.est.2c00738.
20. Nishimura, S., Kimiwada, K., Yagioka, A., Hayashi, S., and Oka, N. (2020). Effect of intermittent drainage in reduction of methane emission from paddy soils in Hokkaido, northern Japan. Soil Sci. Plant Nutr. *66*, 360–368. https://doi.org/10.1080/00380768.2019.1706191.
21. Song, H.J., Lee, J.H., Jeong, H.C., Choi, E.J., Oh, T.K., Hong, C.O., and Kim, P.J. (2019). Effect of straw incorporation on methane emission in rice paddy: conversion factor and smart straw management. Appl. Biol. Chem. *62*, 1–13. https://doi.org/10.1186/s13765-019-0476-7.
22. Sander, B.O., Schneider, P., Romasanta, R., Samoy-Pascual, K., Sibayan, E.B., Asis, C.A., and Wassmann, R. (2020). Potential of alternate wetting and drying irrigation practices for the mitigation of ghg emissions from rice fields: two cases in Central Luzon (Philippines). Agriculture *10*, 350. https://doi.org/10.3390/agriculture10080350.
23. Setyanto, P., Pramono, A., Adriany, T.A., Susilawati, H.L., Tokida, T., Padre, A.T., and Minamikawa, K. (2018). Alternate wetting and drying reduces methane emission from a rice paddy in Central Java, Indonesia without yield loss. Soil Sci. Plant Nutr. *64*, 23–30. https://doi.org/10.1080/00380768.2017.1409600.
24. Yan, X., Yagi, K., Akiyama, H., and Akimoto, H. (2005). Statistical analysis of the major variables controlling methane emission from rice fields. Global Change Biol. *11*, 1131–1141. https://doi.org/10.1111/j.1365-2486.2005.00976.x.
25. Takakai, F., Kominami, Y., Ohno, S., and Nagata, O. (2020). Effect of the long-term application of organic matter on soil carbon accumulation and GHG emissions from a rice paddy field in a cool-temperate region, Japan. I. Comparison of rice straw and rice straw compost. Soil Sci. Plant Nutr. *66*, 84–95. https://doi.org/10.1080/00380768.2019.1609335.
26. Gupta, K., Kumar, R., Baruah, K.K., Hazarika, S., Karmakar, S., and Bordoloi, N. (2021). Greenhouse gas emission from rice fields: a review from Indian context. Environ. Sci. Pollut. Res. Int. *28*, 30551–30572. https://doi.org/10.1007/s11356-021-13935-1.
27. Bharali, A., Baruah, K.K., and Gogoi, N. (2017). Methane emission from irrigated rice ecosystem: relationship with carbon fixation, partitioning and soil carbon storage. Paddy Water Environ. *15*, 221–236. https://doi.org/10.1007/s10333-016-0541-3.
28. Li, C., Frolking, S., and Frolking, T.A. (1992). A model of nitrous oxide evolution from soil driven by rainfall events: 1. Model structure and sensitivity. J. Geophys. Res. *97*, 9759–9776. https://doi.org/10.1029/92JD00509.
29. Parton, W.J., Hartman, M., Ojima, D., and Schimel, D. (1998). DAYCENT and its land surface submodel: description and testing. Global Planet. Change *19*, 35–48. https://doi.org/10.1016/S0921-8181(98)00040-X.
30. Ren, W., Tian, H., Xu, X., Liu, M., Lu, C., Chen, G., Melillo, J., Reilly, J., Liu, J., and Liu, J. (2011). Spatial and temporal patterns of CO2 and CH4 fluxes in China's croplands in response to multifactor environmental changes. Tellus B *63*, 222–240. https://doi.org/10.1111/j.1600-0889.2010.00522.x.
31. Cai, Z., Sawamoto, T., Li, C., Kang, G., Boonjawat, J., Mosier, A., Wassmann, R., Tsuruta, H., and Tsuruta, H. (2003). Field validation of the DNDC model for greenhouse gas emissions in East Asian cropping systems. Global Biogeochem. Cycles *17*. https://doi.org/10.1029/2003GB002046.
32. Cheng, K., Ogle, S.M., Parton, W.J., and Pan, G. (2013). Predicting methanogenesis from rice paddies using the DAYCENT ecosystem model. Ecol. Model. *261–262*, 19–31. https://doi.org/10.1016/j.ecolmodel.2013.04.003.
33. Huang, Y., Zhang, W., Zheng, X., Li, J., and Yu, Y. (2004). Modeling methane emission from rice paddies with various agricultural practices. J. Geophys. Res. *109*. https://doi.org/10.1029/2003JD004401.
34. Katayanagi, N., Fumoto, T., Hayano, M., Shirato, Y., Takata, Y., Leon, A., and Yagi, K. (2017). Estimation of total CH4 emission from Japanese rice paddies using a new estimation method based on the DNDC-Rice simulation model. Sci. Total Environ. 346–355. https://doi.org/10.1016/j.scitotenv.2017.05.090.
35. Zhang, B., Tian, H., Ren, W., Tao, B., Lu, C., Yang, J., Banger, K., Pan, S., and Pan, S. (2016). Methane emissions from global rice fields: Magnitude, spatiotemporal patterns, and environmental controls. Global Biogeochem. Cycles *30*, 1246–1263. https://doi.org/10.1002/2016GB005381.
36. Qian, H., Zhu, X., Huang, S., Linquist, B., Kuzyakov, Y., Wassmann, R., Minamikawa, K., Martinez-Eixarch, M., Yan, X., Zhou, F., et al. (2023). Greenhouse gas emissions and mitigation in rice agriculture. Sci. Total Environ. *4*, 716–732. https://doi.org/10.1038/s43017-023-00482-1.
37. Minamikawa, K., Sakai, N., and Yagi, K. (2006). Methane emission from paddy fields and its mitigation options on a field scale. Microb. Environ. *21*, 135–147. https://doi.org/10.1264/jsme2.21.135.
38. Denier van Der Gon, H.A.C., Kropff, M.J., Van Breemen, N., Wassmann, R., Lantin, R.S., Aduna, E., Corton, T.M., Van Laar, H.H., and Van Laar, H.H. (2002). Optimizing grain yields reduces CH4 emissions from rice paddy fields. Proc. Natl. Acad. Sci. USA *99*, 12021–12024. https://doi.org/10.1073/pnas.192276599.
39. Su, J., Hu, C., Yan, X., Jin, Y., Chen, Z., Guan, Q., Wang, Y., Zhong, D., Jansson, C., Wang, F., et al. (2015). Expression of barley SUSIBA2 transcription factor yields high-starch low-methane rice. Nature *523*, 602–606. https://doi.org/10.1038/nature14673.
40. Nan, Q., Xin, L., Qin, Y., Waqas, M., and Wu, W. (2021). Exploring long-term effects of biochar on mitigating methane emissions from paddy soil: a review. Biochar *3*, 125–134. https://doi.org/10.1007/s42773-021-00096-0.
41. Shackley, S., Hammond, J., Gaunt, J., and Ibarrola, R. (2011). The feasibility and costs of biochar deployment in the UK. Carbon Manag. *2*, 335–356. https://doi.org/10.4155/cmt.11.22.
42. Galinato, S.P., Yoder, J.K., and Granatstein, D. (2011). The economic value of biochar in crop production and carbon sequestration. Energy Pol. *39*, 6344–6350. https://doi.org/10.1016/j.enpol.2011.07.035.
43. Kung, C.C., McCarl, B.A., and Cao, X. (2013). Economics of pyrolysis-based energy production and biochar utilization: A case study in Taiwan. Energy Pol. *60*, 317–323. https://doi.org/10.1016/j.enpol.2013.05.029.
44. Parker, R., and Boesch, H. (2020). University of Leicester GOSAT Proxy XCH4 v9.0. Centre for Environmental Data Analysis *12*, 3383–3412. https://doi.org/10.5285/18ef8247f52a4cb6a14013f8235cc1eb.
45. Janssens-Maenhout, G., Crippa, M., Guizzardi, D., Muntean, M., Schaaf, E., Dentener, F., Bergamaschi, P., Pagliari, V., Olivier, J.G.J., Peters, J.A.H.W., et al. (2019). EDGAR v4. 3.2 Global Atlas of the three major greenhouse gas emissions for the period 1970–2012. Earth Syst. Sci. Data *11*, 959–1002. https://doi.org/10.5194/essd-11-959-2019.
46. FAOSTAT (2022). FAOSTAT statistical database (Food and Agriculture Organization of the United Nations). https://www.fao.org/faostat/en/#data.
47. Pramono, A., Adriany, T.A., Yulianingsih, E., Sopiawati, T., and Hervani, A. (2021). Combined compost with biochar application to mitigate greenhouse gas emission in paddy field. IOP Conf. Ser. Earth Environ. Sci. *653*, 012109. https://doi.org/10.1088/1755-1315/653/1/012109.
48. Gorh, D., and Baruah, K.K. (2019). Estimation of methane and nitrous oxide emission from wetland rice paddies with reference to global warming potential. Environ. Sci. Pollut. Res. Int. *26*, 16331–16344. https://doi.org/10.1007/s11356-019-05026-z.
49. Wang, J., Yao, X., Jia, Z., Zhu, L., Zheng, P., Kartal, B., and Hu, B. (2022). Nitrogen input promotes denitrifying methanotrophs'

abundance and contribution to methane emission reduction in coastal wetland and paddy soil. Environ. Pollut. *302*, 119090. https://doi.org/10.1016/j.envpol.2022.119090.

50. Singh, J.S., and Strong, P.J. (2016). Biologically derived fertilizer: a multifaceted bio-tool in methane mitigation. Ecotoxicol. Environ. Saf. *124*, 267–276. https://doi.org/10.1016/j.ecoenv.2015.10.018.
51. Malyan, S.K., Bhatia, A., Fagodiya, R.K., Kumar, S.S., Kumar, A., Gupta, D.K., Tomer, R., Harit, R.C., Kumar, V., Jain, N., et al. (2021). Plummeting global warming potential by chemicals interventions in irrigated rice: A lab to field assessment. Agric. Ecosyst. Environ. *319*, 107545. https://doi.org/10.1016/j.agee.2021.107545.
52. Sun, B.F., Zhao, H., LÜ, Y.Z., Lu, F., and Wang, X.K. (2016). The effects of nitrogen fertilizer application on methane and nitrous oxide emission/uptake in Chinese croplands. J. Integr. Agric. *15*, 440–450. https://doi.org/10.1016/S2095-3119(15)61063-2.
53. Toma, Y., Takechi, Y., Inoue, A., Nakaya, N., Hosoya, K., Yamashita, Y., Adachi, M., Kono, T., Hideto, U., and Hideto, U. (2021). Early mid-season drainage can mitigate greenhouse gas emission from organic rice farming with green manure application. Soil Sci. Plant Nutr. *67*, 482–492. https://doi.org/10.1080/00380768.2021.1927832.
54. Chen, Z., Balasus, N., Lin, H., Nesser, H., and Jacob, D.J. (2024). African rice cultivation linked to rising methane. Nat. Clim. Change *14*, 148–151. https://doi.org/10.1038/s41558-023-01907-x.
55. Yin, X., Song, Z., Shi, S., Bai, Z., Jiang, Y., Zheng, A., Huang, W., Chen, N., Chen, F., and Chen, F. (2024). Developments and prospects of multiple cropping in China. Farming System *2*, 100083. https://doi.org/10.1016/j.farsys.2024.100083.
56. Zhang, X., Bi, J., Sun, H., Zhang, J., and Zhou, S. (2019). Greenhouse gas mitigation potential under different rice-crop rotation systems: from site experiment to model evaluation. Clean Technol. Environ. Policy *21*, 1587–1601. https://doi.org/10.1007/s10098-019-01729-6.
57. Zhang, Z., Fan, J., Wan, Y., Wang, J., Liao, Y., Lu, Y., and Qin, X. (2023). Evaluation of Methane Emission Reduction Potential of Water Management and Chinese Milk Vetch Planting in Hunan Paddy Rice Fields. Agronomy *13*, 1799. https://doi.org/10.3390/agronomy13071799.
58. Bo, Y., Jägermeyr, J., Yin, Z., Jiang, Y., Xu, J., Liang, H., and Zhou, F. (2022). Global benefits of non-continuous flooding to reduce greenhouse gases and irrigation water use without rice yield penalty. Global Change Biol. *28*, 3636–3650. https://doi.org/10.1111/gcb.16132.
59. Souza, R., Yin, J., and Calabrese, S. (2021). Optimal drainage timing for mitigating methane emissions from rice paddy fields. Geoderma *394*, 114986. https://doi.org/10.1016/j.geoderma.2021.114986.
60. Zhou, L.Y., Zhu, Y.H., Kan, Z.R., Li, F.M., and Zhang, F. (2023). The impact of crop residue return on the food–carbon–water–energy nexus in a rice–wheat rotation system under climate warming. Sci. Total Environ. *894*, 164675. https://doi.org/10.1016/j.scitotenv.2023.164675.
61. Hu, N.J., Han, X.Z., Yang, M.F., Zhang, Z.W., Bian, X.M., and Zhu, L.Q. (2015). Short-term influence of straw return on the contents of soil organic carbon fractions, enzyme activities and crop yieldsin rice-wheat rotation farmland. J. Plant Nutr. Fert. *21*, 371–377. https://doi.org/10.11674/zwyf.2015.0211.
62. Hung, D.T., Banfield, C.C., Dorodnikov, M., and Sauer, D. (2022). Improved water and rice residue managements reduce greenhouse gas emissions from paddy soil and increase rice yields. Paddy Water Environ. *20*, 93–105. https://doi.org/10.1007/s10333-021-00877-0.
63. Xie, B., Zhou, Z., Zheng, X., Zhang, W., and Zhu, J. (2010). Modeling methane emissions from paddy rice fields under elevated atmospheric carbon dioxide conditions. Adv. Atmos. Sci. *27*, 100–114. https://doi.org/10.1007/s00376-009-8178-4.
64. Huang, Y., Sass, R., and Fisher, F. (1997). Methane emission from Texas rice paddy soils. 1. Quantitative multi-year dependence of CH4 emission on soil, cultivar and grain yield. Global Change Biol. *3*, 479–489. https://doi.org/10.1046/j.1365-2486.1997.00083.x.
65. Huang, Y., Sass, R., and Fisher, F. (1997). Methane emission from Texas rice paddy soils. 2. Seasonal contribution of rice biomass production to CH4 emission. Global Change Biol. *3*, 491–500. https://doi.org/10.1046/j.1365-2486.1997.00106.x.
66. Kongchum, M., Bollich, P.K., Hudnall, W.H., DeLaune, R.D., and Lindau, C.W. (2006). Decreasing methane emission of rice by better crop management. Agron. Sustain. Dev. *26*, 45–54. https://doi.org/10.1051/agro:2005056.
67. Wassmann, R., Buendia, L.V., Lantin, R.S., Bueno, C.S., Lubigan, L.A., Umali, A., Nocon, N., Javellana, A., Neue, H., and Neue, H.U. (2000). Mechanisms of crop management impact on methane emissions from rice fields in Los Baños, Philippines. Nutr. Cycl. Agroecosyst. *58*, 107–119. https://doi.org/10.1023/A:1009838401699.
68. Vu, Q.D., de Neergaard, A., Tran, T.D., Hoang, Q.Q., Ly, P., Tran, T.M., and Jensen, L.S. (2015). Manure, biogas digestate and crop residue management affects methane gas emissions from rice paddy fields on Vietnamese smallholder livestock farms. Nutr. Cycl. Agroecosyst. *103*, 329–346. https://doi.org/10.1007/s10705-015-9746-x.
69. Digitizer, I.P. (2020). How to Extract Data from Graphs using Plot Digitizer or Getdata Graph Digitizer. http://www.getdata-graph-digitizer.com/.
70. FAO/IIASA/ISRIC/ISSCAS/JRC (2012). Harmonized World Soil Database (Version 1.2) (Rome, Italy and IIASA, Laxenburg, Austria: FAO). https://www.fao.org/soils-portal/data-hub/soil-maps-and-databases/harmonized-world-soil-database-v12/en/.
71. Hersbach, H., Bell, B., Berrisford, P., Biavati, G., Horányi, A., Muñoz Sabater, J., Nicolas, J., Peubey, C., Radu, R., Rozum, I., et al. (2023). ERA5 hourly data on single levels from 1940 to present. Copernicus Climate Change Service (C3S) Climate Data Store (CDS). https://doi.org/10.24381/cds.adbb2d47.
72. Monfreda, C., Ramankutty, N., and Foley, J.A. (2008). Farming the planet: 2. Geographic distribution of crop areas, yields, physiological types, and net primary production in the year 2000. Global Biogeochem. Cycles *22*, GB1022. https://doi.org/10.1029/2007GB002947.
73. Vicente-Serrano, S.M., Saz-Sánchez, M.A., and Cuadrat, J.M. (2003). Comparative analysis of interpolation methods in the middle Ebro Valley (Spain): application to annual precipitation and temperature. Clim. Res. *24*, 161–180. https://doi.org/10.3354/cr024161.
74. Haque, M.M., Biswas, J.C., Maniruzaman, M., Akhter, S., and Kabir, M.S. (2020). Carbon sequestration in paddy soil as influenced by organic and inorganic amendments. Carbon Manag. *11*, 231–239. https://doi.org/10.1080/17583004.2020.1738822.
75. Pandey, A., Mai, V.T., Vu, D.Q., Bui, T.P.L., Mai, T.L.A., Jensen, L.S., and de Neergaard, A. (2014). Organic matter and water management strategies to reduce methane and nitrous oxide emissions from rice paddies in Vietnam. Agric. Ecosyst. Environ. *196*, 137–146. https://doi.org/10.1016/j.agee.2014.06.010.
76. Oo, A.Z., Sudo, S., Inubushi, K., Chellappan, U., Yamamoto, A., Ono, K., Mano, M., Hayashida, S., Koothan, V., Osawa, T., et al. (2018). Mitigation potential and yield-scaled global warming potential of early-season drainage from a rice paddy in Tamil Nadu, India. Agronomy *8*, 202. https://doi.org/10.3390/agronomy8100202.
77. Meijide, A., Gruening, C., Goded, I., Seufert, G., and Cescatti, A. (2017). Water management reduces greenhouse gas emissions in a Mediterranean rice paddy field. Agric. Ecosyst. Environ. *238*, 168–178. https://doi.org/10.1016/j.agee.2016.08.017.
78. Nugroho, S.G., Sunyoto, Lumbanraja, J., Suprapto, H., Ardjasa, W.S., and Kimura, M. (1997). Effect of rice variety on methane emission from an Indonesian paddy field. Soil Sci. Plant Nutr. *43*, 799–809. https://doi.org/10.1080/00380768.1997.10414646.
79. Bayer, C., Costa, F.d.S., Pedroso, G.M., Zschornack, T., Camargo, E.S., Lima, M.A.d., Frigheto, R.T., Gomes, J., Marcolin, E., Macedo, V.R.M., and Macedo, V.R.M. (2014). Yield-scaled greenhouse gas emissions from flood irrigated rice under long-term conventional tillage and no-till systems in a Humid Subtropical climate. Field Crops Res. *162*, 60–69. https://doi.org/10.1016/j.fcr.2014.03.015.
80. Jermsawatdipong, P., Murase, J., Prabuddham, P., Hasathon, Y., Khomthong, N., Naklang, K., Watanabe, A., Haraguchi, H., Kimura, M., and Kimura, M. (1994). Methane emission from plots with differences in fertilizer application in Thai paddy fields. Soil Sci. Plant Nutr. *40*, 63–71. https://doi.org/10.1080/00380768.1994.10414279.
81. Lauren, J.G., Pettygrove, G.S., and Duxbury, J.M. (1994). Methane emissions associated with a green manure amendment to flooded rice in California. Biogeochemistry *24*, 53–65. https://doi.org/10.1007/BF02390179.
82. Lee, C.H., Park, K.D., Jung, K.Y., Ali, M.A., Lee, D., Gutierrez, J., and Kim, P.J. (2010). Effect of Chinese milk vetch (Astragalus sinicus L.) as a green manure on rice productivity and methane emission in paddy soil. Agric. Ecosyst. Environ. *138*, 343–347. https://doi.org/10.1016/j.agee.2010.05.011.
83. Debnath, G., Jain, M.C., Kumar, S., Sarkar, K., and Sinha, S.K. (1996). Methane emissions from rice fields amended with biogas slurry and farm yard manure. Clim.

Change *33*, 97–109. https://doi.org/10.1007/BF00140515.

84. Datta, A., Yeluripati, J.B., Nayak, D.R., Mahata, K.R., Santra, S.C., and Adhya, T.K. (2013). Seasonal variation of methane flux from coastal saline rice field with the application of different organic manures. Atmos. Environ. X. *66*, 114–122. https://doi.org/10.1016/j.atmosenv.2012.06.008.
85. Singh, S., Singh, J.S., and Kashyap, A.K. (1999). Methane flux from irrigated rice fields in relation to crop growth and N-fertilization. Soil Biol. Biochem. *31*, 1219–1228. https://doi.org/10.1016/S0038-0717(99)00027-9.
86. Kim, G.Y., Gutierrez, J., Jeong, H.C., Lee, J.S., Haque, M.D.M., and Kim, P.J. (2014). Effect of intermittent drainage on methane and nitrous oxide emissions under different fertilization in a temperate paddy soil during rice cultivation. J. Korean Soc. Appl. Biol. Chem. *57*, 229–236. https://doi.org/10.1007/s13765-013-4298-8.
87. Xia, L., Xia, Y., Ma, S., Wang, J., Wang, S., Zhou, W., and Yan, X. (2016). Greenhouse gas emissions and reactive nitrogen releases from rice production with simultaneous incorporation of wheat straw and nitrogen fertilizer. Biogeosciences *13*, 4569–4579. https://doi.org/10.5194/bg-13-4569-2016.
88. Li, X., Ma, J., Yao, Y., Liang, S., Zhang, G., Xu, H., and Yagi, K. (2014). Methane and nitrous oxide emissions from irrigated lowland rice paddies after wheat straw application and midseason aeration. Nutr. Cycl. Agroecosyst. *100*, 65–76. https://doi.org/10.1007/s10705-014-9627-8.
89. Zhang, Z.S., Cao, C.G., Guo, L.J., and Li, C.F. (2016). Emissions of CH 4 and CO 2 from paddy fields as affected by tillage practices and crop residues in central China. Paddy Water Environ. *14*, 85–92. https://doi.org/10.1007/s10333-015-0480-4.
90. Ma, J., Li, X.L., Xu, H., Han, Y., Cai, Z.C., and Yagi, K. (2007). Effects of nitrogen fertiliser and wheat straw application on CH4 and N2O emissions from a paddy rice field. Soil Res. *45*, 359–367. https://doi.org/10.1071/SR07039.
91. Ma, J., Xu, H., Yagi, K., and Cai, Z. (2008). Methane emission from paddy soils as affected by wheat straw returning mode. Plant Soil *313*, 167–174. https://doi.org/10.1007/s11104-008-9689-y.
92. Ly, P., Jensen, L.S., Bruun, T.B., and de Neergaard, A. (2013). Methane (CH_4) and nitrous oxide (N_2O) emissions from the system of rice intensification (SRI) under a rain-fed lowland rice ecosystem in Cambodia. Nutr. Cycl. Agroecosyst. *97*, 13–27. https://doi.org/10.1007/s10705-013-9588-3.
93. Minamikawa, K., and Sakai, N. (2006). The practical use of water management based on soil redox potential for decreasing methane emission from a paddy field in Japan. Agric. Ecosyst. Environ. *116*, 181–188. https://doi.org/10.1016/j.agee.2006.02.006.
94. Oo, A.Z., Sudo, S., Fumoto, T., Inubushi, K., Ono, K., Yamamoto, A., Bellingrath-Kimura, S.D., Win, K.T., Umamageswari, C., Bama, K.S., et al. (2020). Field validation of the DNDC-rice model for methane and nitrous oxide emissions from double-cropping paddy rice under different irrigation practices in Tamil Nadu, India. Agriculture *10*, 355. https://doi.org/10.3390/agriculture10080355.
95. Setyanto, P., Makarim, A.K., Fagi, A.M., Wassmann, R., and Buendia, L.V. (2000). Crop management affecting methane emissions from irrigated and rainfed rice in Central Java (Indonesia). Nutr. Cycl. Agroecosyst. *58*, 85–93. https://doi.org/10.1023/A:1009834300790.
96. Corton, T.M., Bajita, J.B., Grospe, F.S., Pamplona, R.R., Assis Jr, C., Wassmann, R., Lantin, R., Buendia, L.V., and Buendia, L.V. (2000). Methane emission from irrigated and intensively managed rice fields in Central Luzon (Philippines). Nutr. Cycl. Agroecosyst. *58*, 37–53. https://doi.org/10.1023/A:1009826131741.
97. Zhang, G., Yu, H., Fan, X., Yang, Y., Ma, J., and Xu, H. (2016). Drainage and tillage practices in the winter fallow season mitigate CH_4 and N_2O emissions from a double-rice field in China. Atmos. Chem. Phys. *16*, 11853–11866. https://doi.org/10.5194/acp-16-11853-2016.
98. Nugroho, S.G., Lumbanraja, J., Suprapto, H., Kimura, M., Sunyoto, and Haraguchi, H. (1996). Three-year measurement of methane emission from an Indonesian paddy field. Plant Soil *181*, 287–293. https://doi.org/10.1007/BF00012063.
99. Shang, Q., Yang, X., Gao, C., Wu, P., Liu, J., Xu, Y., Shen, Q., Zou, J., Guo, S., and Guo, S. (2011). Net annual global warming potential and greenhouse gas intensity in Chinese double rice-cropping systems: a 3-year field measurement in long-term fertilizer experiments. Global Change Biol. *17*, 2196–2210. https://doi.org/10.1111/j.1365-2486.2010.02374.x.
100. Uno, K., Ishido, K., Nguyen Xuan, L., Nguyen Huu, C., and Minamikawa, K. (2021). Multiple drainage can deliver higher rice yield and lower methane emission in paddy fields in An Giang Province, Vietnam. Paddy Water Environ. *19*, 623–634. https://doi.org/10.1007/s10333-021-00861-8.
101. Li, C., Qiu, J., Frolking, S., Xiao, X., Salas, W., Moore, B., III, Boles, S., Huang, Y., Sass, R., and Sass, R. (2002). Reduced methane emissions from large-scale changes in water management of China's rice paddies during 1980–2000. Geophys. Res. Lett. *29*, 33-1–33-4. https://doi.org/10.1029/2002GL015370.
102. Kendall, M.G., and Stuart, A. (1969). The Advanced Theory of Statistics. Biometrics *3*, 435. https://doi.org/10.2307/2528806.
103. FAO (2022). World Food and Agriculture – Statistical Yearbook 2022 (Rome: FAO). https://doi.org/10.4060/cc2211en.
104. Waha, K., Dietrich, J.P., Portmann, F.T., Siebert, S., Thornton, P.K., Bondeau, A., and Herrero, M. (2020). Multiple cropping systems of the world and the potential for increasing cropping intensity. Global Environ. Change *64*, 102131. https://doi.org/10.1016/j.gloenvcha.2020.102131.
105. Laborte, A.G., Gutierrez, M.A., Balanza, J.G., Saito, K., Zwart, S.J., Boschetti, M., Murty, M.V.R., Villano, L., Aunario, J.K., Reinke, R., et al. (2017). RiceAtlas, a spatial database of global rice calendars and production. Sci. Data *4*, 1–10. https://doi.org/10.1038/sdata.2017.74.
106. McCuen, R.H., Knight, Z., and Cutter, A.G. (2006). Evaluation of the Nash–Sutcliffe efficiency index. J. Hydrol. Eng. *11*, 597–602. https://doi.org/10.1061/(ASCE)1084-0699(2006)11:6(597.
107. Gupta, H.V., and Kling, H. (2011). On typical range, sensitivity, and normalization of Mean Squared Error and Nash-Sutcliffe Efficiency type metrics. Water Resour. Res. *47*. https://doi.org/10.1029/2011WR010962.
108. Xu, Y., Knudby, A., Shen, Y., and Liu, Y. (2018). Mapping monthly air temperature in the Tibetan Plateau from MODIS data based on machine learning methods. IEEE J. Sel. Top. Appl. Earth Obs. Remote Sens. *11*, 345–354. https://doi.org/10.1109/JSTARS.2017.2787191.
109. Moriasi, D.N., Arnold, J.G., Van Liew, M.W., Bingner, R.L., Harmel, R.D., and Veith, T.L. (2007). Model evaluation guidelines for systematic quantification of accuracy in watershed simulations. Trans. ASABE *50*, 885–900. https://doi.org/10.13031/2013.23153.

STAR★METHODS

KEY RESOURCES TABLE

REAGENT or RESOURCE	SOURCE	IDENTIFIER
Deposited data		
Global rice field observation dataset	Google Scholar	Supplementary Excel
Ratio of various water regimes	Yan et al.[14]	https://doi.org/10.1029/2008GB003299
Air temperature	EAR5	https://cds.climate.copernicus.eu/cdsapp#!/dataset/reanalysis-era5-single-levels?tab=overview
Soil sand fraction	HWSD	http://webarchive.iiasa.ac.at/Research/LUC/External-World-soil-database/HTML/HWSD_Data.html?sb=4
Rice harvested area distribution	EarthStat	http://www.Earthstat.org/
Rice harvested area statistics	FAO	https://www.fao.org/faostat/en/#data/
Rice yield distribution	EarthStat	http://www.Earthstat.org/
Rice yield distribution	FAO	https://www.fao.org/faostat/en/#data/
Rice rotation	Waha et al.[104]	https://doi.org/10.25919/5f1f7bb3270bb
Rice phenology	RiceAtlas	https://doi.org/10.7910/DVN/JE6R2R
Software and algorithms		
ArcGIS	ESRI	https://www.esri.com/en-us/arcgis/about-arcgis/overview
Origin	OriginLab	https://www.originlab.com/
MATLAB	MathWorks	https://www.mathworks.com/products/matlab.html
Microsoft Excel	Microsoft	https://www.microsoft.com/en-us/microsoft-365/excel

METHOD DETAILS

CH4MOD model

Overview

CH4MOD is a process-based model that can be used to simulate CH_4 production, oxidation, and emissions in rice paddies under various environmental conditions and agricultural management practices.[13,33,63] The rationale of this model is that CH_4 production rates are determined by the availability of methanogenic substrates and the influences of environmental factors, e.g., soil temperature, soil texture, and soil redox potential (*Eh*). Methanogenic substrates are mainly derived from the rice root exudation and added OM (including crop residues and organic fertilizers). CH_4 is transported via rice aerenchyma and ebullition. CH_4 oxidation occurs during plant transport and increases as plants grow.

The CH4MOD model runs on a daily time step. Model inputs include air temperature, percentage of sand (0.2–2 mm) (*SAND*), rice grain yield (*GY*), type and amount of OM amendment (*OM*), and type of water regime used for rice irrigation (*IRRI*). OM applied in rice fields includes animal manure, green manure, biogas residue, and crop straw. Crop roots and stubble (approximately 10% of the aboveground biomass) of the previous season are considered buried in the soil as an OM amendment. The initial nonstructural (OM_N) and structural (OM_S) fractions of the different types of *OM* are summarized in Table S1. Currently, the classification of water regimes in this model primarily involves three states: F for flooding, D for draining, and M for intermittent irrigation. Each state determines the *Eh* changes. Under flooding conditions, the *Eh* value continually decreases and promotes CH_4 production, while this process sharply decreases due to the high *Eh* values under drainage conditions. Intermittent irrigation always occurs at the end of the growth stage, and *Eh* remains nearly constant. The combination of these three states results in five distinct water regimes, i.e., F, FDFM, FDM, FM, and M, considered in the original model. More details on the model are described in previous studies.[13,33,64,65]

In this study, we followed the overall model framework and calibration but made a few modifications to fit the global validation. Firstly, since the model was calibrated and validated in most countries without India, the country with the largest distribution of rice paddies in the world, we recalibrated the rice variety index (VI) for India. In addition, a new water regime, FDF, is included, accounting for the water

regime in the USA, Philippines, Vietnam, etc.[66–68] Table S2 provides a detailed description of the six water regimes. The specific mechanistic equations and model variables are provided in supplement S1, Table S3 and S4.

Site information and data sources

Site-level CH_4 flux observations from rice paddies worldwide were used to parameterize and validate the CH4MOD model. The dataset of Wang et al.[10] was updated and expanded to incorporate CH_4 emission observational data from rice fields available worldwide. Recent relevant studies have included variables such as site location, yield, aboveground biomass, soil sand content, rice phenology, variety, and straw return rate. In this study, published CH_4 field measurement studies up to 2022 were comprehensively searched. The studies were ranked by relevance based on the following: (1) observations covering the entire cultivation period from sowing/transplanting to harvesting; (2) information including location, crop (yield, biomass, variety, and rotation), and management practice (water regime and fertilization); and (3) only experiments in rice fields were considered, while other experiments such as incubation in the laboratory were excluded. A total of 141 publications with 1288 CH_4 flux observations covering 97 sites in rice fields were obtained (Table S5 in the Excel Supplement). The new datasets contain field measurements covering the main rice cultivation regions across the world, including China, India, Bangladesh, Brazil, Cambodia, Indonesia, Italy, Japan, the Philippines, South Korea, Spain, Thailand, Uruguay, the USA, and Vietnam, spanning the 1990 to 2019 period (below figure). The measurements also covered different water regimes, OM amendments, rice varieties, and rice cropping systems.

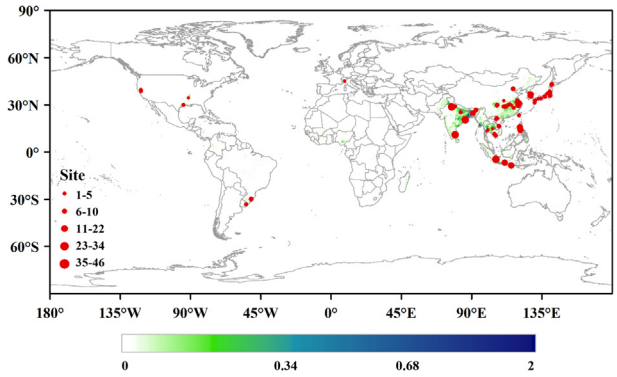

Rice paddy site distribution

The size of the red dots reflects the number of experiments conducted at that site. The base map shows the average fractional proportion of the harvested area to the grid area from 1997 to 2003[72].

For each study, the metadata (year published and last name of the first author), time (year and date), and location (longitude and latitude) of the field experiments; rice characteristics (variety, yield, biomass, length of the cultivation period, transplant and harvest dates, and rotation); soil sand percentage; agricultural management practices (water regime during and before the rice-growing season and types and amount of OM amendment); and average CH_4 flux during the rice-growing season as well as the seasonal total CH_4 fluxes were compiled. Finally, 986 CH_4 flux observations with complete information were retained. Data contained in tables and the text were extracted by transcription, while the graphically presented data were extracted using GetData Graph Digitizer software.[69]

Missing soil sand percentage values at a few sites were acquired from the 30″ × 30″ resolution HWSD global soil dataset within the 0–30 cm range based on the latitude and longitude.[70] Air temperature data for the experimental observations was largely unavailable. Therefore, location data and time information were used to extract data from the ERA5 global daily dataset at a resolution of 0.25°.[71]

MODEL PARAMETERIZATION

There are a number of constant, management-specific, or crop-specific parameters in the CH4MOD model (Tables S3 and S4). In this study, the values of most parameters remained unchanged since the model was primarily parameterized and validated across China and the United States in previous studies,[13,33] as well as sporadic validations performed in Italy, Indonesia, and the Philippines for flooded rice paddies without OM amendments. However, the CH4MOD model has not been parametrized and validated for India, which is the leading rice-harvesting area in the world.

The variety index *(VI)* represents the relative difference in the CH_4 production capability among rice cultivars. Huang et al. (1997)[64] calculated its value based on site observations in China, Italy, Indonesia, the Philippines, and the United States. Considering the differences in yields and rice varieties, the *VI* parameter in India was recalculated in this study. Following Huang et al. (1997),[64] the *VI* parameter can be defined as follows:

$$VI = \frac{(E/GY)/SI}{RRATIO} \quad \text{(Equation 1)}$$

where *E* denotes the seasonal CH_4 flux (g/m^2), *GY* is the grain yield (g/m^2), and *SI* is the soil index (dimensionless) calculated by the soil sand percentage (Equation S11). *RRATIO* is the average value of (*E/GY*)/*SI_avg*, which denotes the reference value of *E/GY* under the mean soil sand percentage in India. This calculation was based on 46 cases (noted in Table S5) with continuous flooding and without OM amendment in India, among which 15 cases (representing approximately the mean soil sand percentage) were used to calculate *RRATIO*. The calculated *VI* value is 0.78, indicating a lower capability than that in other countries (1.0). Figure S1 compares the simulation results before and after this adjustment. It should be noted that we did not exclude these 70 cases in the validation process since this calculation process is independent of the model. Further, we used geographic information systems (GIS) technology to assign a uniform *VI* value to all grid points within a country.

MODEL VALIDATION

The CH4MOD model was then validated by comparing the daily CH_4 fluxes for 30 representative observations and the seasonal total CH_4 emissions for 986 observations globally between the observations and simulations. The total observed and simulated seasonal CH_4 fluxes were determined as the summation of daily values. Missing daily observed CH_4 fluxes were calculated via linear interpolation between two adjacent fluxes. Thirty representative observations (below table) covering different climate and soil conditions, water regimes, OM amendments, and rice cropping systems were selected for validating the seasonal variations in CH_4 fluxes. Four quantitative statistical metrics were used to evaluate the model performance, including the root-mean-square error (RMSE), mean absolute error (MAE), model coefficient of determination (R^2), and model efficiency (EF).[73,108] A detailed description and equations used to calculate these statistics are provided in quantification and statistical analysis section.

Summary of the site observations used for validating the seasonal variations in CH4MOD

Country	Location	Observation year	PlantD/ MatureD	*IRRI*	*OM*	*SAND* (%)	*GY* (g/m^2)	T_{avg} (T_{min}-T_{max}) (°C)	CH_4 (observe/ simulate) (g/m^2)	Reference
Single rice cultivation										
Bangladesh	24.43°N, 91.37°E	2017	7.1/11.13	F	no	37	273	28.3(22–32)	23.90/23.89	Haque et al.[74]
Vietnam	20.93°N, 105.85°E	2013	2.23/5.31	F	5 t/ha FYM	22	602	25.6(17–33)	35.30/33.27	Pandey et al.[75]
India	11°N, 79.5°E	2017–2018	10.6/1.9	F	1.1 t/ha rice straw	13.6	626	26.8(24–31)	35.93/34.43	Oo et al.[76]
Italy	45.07°N, 8.72°E	2009	4.30/9.20	F	no	47	701	23.5(16–30)	41.46/40.58	Meijide et al.[77]
Indonesia	4.62°S, 105.51°E	1994–1995	12.28/3.29	F	2.5 t/ha rice straw	51	572	26.3(25–27)	51.30/50.73	Nugroho et al.[78]
Brazil	29.9°S, 51.1°W	2002–2003	12.10/4.5	F	3 t/ha green manure	46	731	23.1(17–26)	49.32/53.18	Bayer et al.[79]
Thailand	13.54°N, 99.82°E	1992	8.14/11.26	F	6 t/ha green manure	34	390	26.9(21–29)	78.53/75.84	Jermsawatdipong et al.[80]
USA	38.56°N, 121.5°W	1992	6.20/10.6	F	10 t/ha rice straw	29	945	23.2(18–28)	88.00/83.86	Lauren et al.[81]
South Korea	36.60°N, 128.75°E	2008	6.5/10.4	F	14 t/ha green manure	42	765	23.4(13–30)	137.67/138.99	Lee et al.[82]
India	28.66°N, 77.2°E	1993	7.15/10.27	F	3 t/ha FYM	66	285	28.5(22–34)	4.94/45.73	Debnath et al.[83]
India	20.2°N, 86.5°E	2011	6.16/10.14	F	1.5 t/ha green manure	67	504	28.6(26–30)	11.95/73.99	Datta et al.[84]
India	25.3°N, 83.02°E	1995	7.17/11.14	F	1 t/ha FYM	47	478	27.4(19–31)	22.74/39.8	Singh et al.[85]
India	11°N, 79.5°E	2017	6.16/9.21	FDF	no	13.6	561	30.9(27–34)	5.96/5.49	Oo et al.[76]
South Korea	37.25°N, 126.98°E	2008	5.25/10.13	FDF	2.5 t/ha rice straw	37	631	22.6(12–29)	30.09/27.47	Kim et al.[86]
Japan	37.11°N, 138.27°E	2010	5.14/9.16	FDF	4.55 t/ha FYM	39	502	21.9(9–28)	35.60/34.78	Takakai et al.[25]
China	31.56°N, 120.70°E	2014	6.15/10.25	FDFM	2.88 t/ha wheat straw	32	591	24.4(14–31)	30.72/29.48	Xia et al.[87]
China	31.95°N, 119.16°E	2008	6.22/11.2	FM	3.75 t/ha wheat straw	17	736	24.3(14–31)	23.89/19.84	Li et al.[88]

(*Continued on next page*)

Continued

Country	Location	Observation year	PlantD/ MatureD	*IRRI*	*OM*	*SAND* (%)	*GY* (g/m^2)	T_{avg} (T_{min}-T_{max}) (°C)	CH_4 (observe/ simulate) (g/m^2)	Reference
China	29.85°N, 115.55°E	2011	7.6/10.13	FM	9 t/h rice straw	34	733	25.4(15–33)	54.20/61.19	Zhang et al.[89]
China	31.28°N, 119.90°E	2004	6.11/10.2	FDM	no	29	556	27.2(17–33)	5.16/5.26	Ma et al.[90]
China	31.97°N, 119.30°E	2006	6.27/10.31	FDM	4.8 t/ha wheat straw	17	668	25.1(14–32)	18.5/18.35	Ma et al.[91]
Cambodia	11.51°N, 104.58°E	2011	9.21/12.7	FDM	5.5 t/ha FYM	78	521	27.1(24–29)	21.37/24.91	Ly et al.[92]
Japan	35.9°N, 140.3°E	2003	5.6/9.17	M	no	37	461	22.6(13–29)	6.51/6.32	Minamikawa and Sakai[93]
India	26.41°N, 92.50°E	2016–2017	10.5/1.18	M	1 t/ha rice straw	13.6	609	28.6(26–31)	11.95/10.17	Oo et al.[94]
Indonesia	6.76°S, 111.17°E	1995–1996	10.27/2.18	RFW	no	29	480	26.4(25–29)	5.60/6.73	Setyanto et al.[95]
Double rice cultivation										
Philippines	15.67°N, 120.99°E	1996	1.15/4.22 7.6/10.14	F F	1 t/ha FYM 1 t/ha rice straw +1 t/ha FYM	5.6	741 535	25.1(20–28) 26.1(23–27)	17.8/13.41 35.3/20.89	Corton et al.[96]
Vietnam	21.3°N, 106.02°E	2017	2.24/5.30 6.9/9.2	FM FM	1 t/ha FYM 1 t/ha FYM	28	589 458	24.2(15–30) 29.0(26–32)	7.99/7.53 14.47/14.14	Hung et al.[62]
China	28.25°N, 116.92°E	2010	4.23/7.11 7.16/11.2	FDFM FDFM	1.75 t/ha rice straw no	29	582 683	25.9(15–33) 26.1(16–33)	8.49/9.25 17.96/19.79	Zhang et al.[97]
Indonesia	4.62°S, 105.51°E	1994–1995	12.28/3.29 5.2/8.7	F F	no no	51	592 503	26.3(25–27) 26.9(25–28)	39.80/38.38 29.50/33.12	Nugroho et al.[98]
China	28.91°N, 111.49°E	2007	4.29/7.15 7.19/10.14	F FDF	3 t/ha rice straw 3 t/ha rice straw	16.7	626 540	26.6(18–34) 25.9(17–32)	25.37/26.24 53.94/50.40	Shang et al.[99]
Triple rice cultivation										
Vietnam	10.47°N, 105.3°E	2015–2016	4.22/7.29 8.2/11.24 12.10/3.21	FDM FDM FDM	no	39	782 817 850	29.4(26–32) 28.1(26–29) 27.8(22–29)	10.7/10.27 12.3/13.43 13.4/14.12	Uno et al.[100]

ANALYSIS OF THE SENSITIVITY

A model sensitivity analysis was conducted for changes in the five inputs of the seasonal CH_4 fluxes using baseline experimental data. Variations of ±10% and ±20% in the air temperature (*T*), *OM*, *GY*, and *SAND* were considered to analyze the model sensitivity, while the *IRRI* was used as a categorical quantity to analyze the sensitivity of the model to irrigation methods by varying the type. In addition, the sensitivity to absolute changes in *OM* and *T* was analyzed by considering the actual change range of each variable. Specifically, six assumptions for *OM* were set, ranging from ±50 to ±100 to ±200 g/m^2. This corresponds to an increase or decrease of 9–36% in the straw return rate based on the current global average yield of 460 g/m^2. *T* variations were examined under four scenarios, encompassing the most concerning climate changes of ±1 and ±2°C. The sensitivity of a given factor to the model output was quantified as the ratio of the change in the seasonal CH_4 emissions ($\Delta CH_4 = CH_4 - CH_{4baseline}$) to the change in the baseline CH_4 emissions ($CH_{4baseline}$).

GLOBAL SCENARIO MODELING

Management scenarios

The CH4MOD model was applied globally under different agricultural management scenarios to focus on the sensitivity of CH_4 emissions to different combinations of management practices in different countries and to provide a model foundation and knowledge for predicting the CH_4 mitigation potential. The scenarios were combined by considering different types of water regimes and fractions of straw incorporation, which are common in major rice cultivation regions worldwide. The straw incorporation fraction was set to RF0 (no straw incorporation), RF30 (30% straw incorporation), and RF50 (50% straw incorporation), approximately corresponding to the current global range of major straw return rates.[61] To enable comparison, water regime scenarios based on the IPCC classification were established. The IPCC has provided a coarse water regime classification at the global scale, which includes continuous flooding (CF), single drainage (SD), and multiple drainage (MD). The

MD scenario represents multiple dry periods, including FDFM, FDM, FM, and M, so the average simulations for the above four water regimes were used to represent the CH_4 emissions under the MD scenario (Table S2). In this study, the three scenarios designed assumed that CF, SD, and MD were the only water regimes across the world. The sensible water regime of RATIO,[14] which is a combination of CF, SD, and MD in different countries (below table), was designed as the last scenario.

Water regimes under the RATIO scenario for major rice-producing countries

Country	CF	SD	MD	Source
China	0.2	0	0.8	Li et al.[101]
India	0.3	0.44	0.26	ALGAS report[a]
Indonesia	0.43	0.22	0.35	ALGAS report[a]
Vietnam	1	0	0	ALGAS report[a]
Japan, Republic of Korea, and Bangladesh	0.2	0	0.8	Assumed to be the same as that in China
Other monsoon Asian countries	0.43	0.22	0.35	Assumed to be the same as that in Indonesia
Other countries	0.3	0.44	0.26	Assumed to be the same as that in India

[a]ALGAS, Asia Least-Cost Greenhouse Gas Abatement Strategy. Reports were downloaded from the Website of the Asian Development Bank. The regime classification includes continuous flooding (CF), single drainage (SD), and multiple drainage (MD), with values showing a share of each type.

In total, 12 management scenarios (below table) were established based on the combination of four water management methods and three straw utilization rates. To explain the uncertainty in the scenarios, the coefficient of variation (CV) was introduced[102]:

Twelve scenarios used in the global modeling, with different combinations of straw incorporation and water regime

Scenarios[a]	CF	SD	MD	RATIO
RF0	RF0_CF	RF0_SD	RF0_MD	RF0_RATIO
RF30	RF30_CF	RF30_SD	RF30_MD	RF30_RATIO
RF50	RF50_CF	RF50_SD	RF50_MD	RF50_RATIO

[a]RF0, RF30, and RF50 indicate 0%, 30%, and 50% straw incorporation. CF, SD, MD, and RATIO show continuous flooding, single drainage, multiple drainage, and RATIO scenario in table.

$$CV = \frac{\sqrt{\frac{1}{N}\sum_{i=1}^{N}(X_i - \overline{X})^2}}{\overline{X}} \times 100\% \quad \text{(Equation 2)}$$

where X_i denotes the CH_4 emissions simulated under each scenario, $\overline{X}$ is the mean value of all the scenarios, and N is the total number of scenarios.

SCENARIO-BASED GLOBAL MODELING

The CH4MOD model was run at a daily step and a spatial resolution of 0.5° × 0.5° to simulate the CH_4 fluxes stemming from global rice paddies under the above scenarios (table). The fluxes were multiplied by the rice area in each grid to obtain the CH_4 emissions in each grid. Then, the global annual CH_4 emissions were obtained by aggregating the gridded values. The simulations were conducted separately for single- and double-rice systems. The study period of 2008–2017 was chosen to compare our results to the latest Global Methane Budget.[4]

Spatially explicit data for the daily air temperature, soil sand fraction, rice harvested area, rice yield, rice rotation, phenology, and management scenarios were established. Daily air temperature data was acquired from the ERA5 dataset.[71] The top 0–30 cm soil layer soil sand fraction was obtained from the Harmonized World Soil Database (HWSD) (version 1.21).[70] Gridded rice yield and harvested area from 2008 to 2017 were established based on national-scale statistical rice harvested area and yield data of the FAO,[103] as well as EarthStat, which provides spatial distribution data for the rice harvested area in approximately 2000.[72] The FAO data were used as standard data to calibrate the EarthStat data, and it was assumed that the rice field distribution remained unchanged from 2008 to 2017. The spatial distribution data were scaled proportionally to the statistical data to obtain the global spatial distribution of the rice harvested area and yield from 2008 to 2017 (Figure S2) (Equations 3 and 4).

$$HarvArea_{grid,i,j} = HarvArea_{grid,earthstat,i,j} \times \frac{HarvArea_{FAO,i}}{HarvArea_{earthstat,i}} \quad \text{(Equation 3)}$$

$$Yield_{grid,i,j} = Yield_{grid,earthstat,i,j} \times \frac{Yield_{FAO,i}}{Yield_{earthstat,i}} \quad \text{(Equation 4)}$$

where $HarvArea_{grid,i,j}$ denotes the final gridded area distribution, i denotes a specific country, and j denotes a particular grid within that country. Moreover, $HarvArea_{grid,earthstat,i,j}$ denotes the gridded area distribution from the EarthStat data for a specific country, $HarvArea_{FAO,i}$ denotes the total rice harvested area in a certain country from the FAO data, and $HarvArea_{earthstat,i}$ corresponds to the total rice harvested area in that country from the EarthStat data. The yield was calculated in the same manner.

Single- and double-rice distributions were generated based on global multiple-crop planting system data from Waha[104] (Figure S2). Since triple-cropped rice fields are extremely rare, they were considered double-cropped rice fields in this study.Figure S2shows the spatial distribution of the mean harvested area and yield from 2008 to 2017 for single- and double-cropped rice fields. Rice phenology data were obtained from the province-level phenological data of RiceAtlas.[105] We utilize geographic information systems (GIS) to align the provincial-scale phenological data with the 0.5° spatial grid. In cases where there are differences between RiceAtlas and Waha et al. (2020)[104] in identifying single- or double-rice varieties, the latter was used to match the phenological information in neighboring regions. The matching order prioritized adjacent provinces at the same latitude, followed by other neighboring provinces, and finally provinces with a similar topography within the country. If not available, phenological information from the closest location in terms of the relative distance was selected. Figure S3 shows the global spatial distribution of the phenology of single- and double-rice varieties. The global data drivers for the CH4MOD model are summarized in below table. All of the data were resampled to a 0.5° × 0.5° spatial resolution to facilitate constructing models at the global scale.

Datasets used for global modeling with CH4MOD

Driving data	Source	Spatial resolution	Temporal resolution	Data access
Air temperature	ERA5[71]	0.25°	Hourly	https://cds.climate.copernicus.eu/cdsapp#!/dataset/reanalysis-era5-single-levels?tab=overview
Soil sand fraction	HWSD V1.21[70]	30″	–	http://webarchive.iiasa.ac.at/Research/LUC/External-World-soil-database/HTML/HWSD_Data.html?sb=4
Harvested area	EarthStat,[72] FAO[103]	5′	Annually	http://www.Earthstat.org/ https://www.fao.org/faostat/en/#data/
Yield	EarthStat,[72] FAO[103]	5′	Annually	http://www.Earthstat.org/ https://www.fao.org/faostat/en/#data/
Rotation	Waha et al. (2020)[104]	0.5°	–	https://doi.org/10.25919/5f1f7bb3270bb
Phenology	RiceAtlas[105]	Province	–	https://doi.org/10.7910/DVN/JE6R2R

QUANTIFICATION AND STATISTICAL ANALYSIS

A simple linear regression was applied to assess the correlation between observed and modeled seasonal total CH_4 fluxes (Figure 3; Figure S1), where N represents the total number of observations in the region. The F-test was used to test whether the regression model was statistically significant overall.

Four quantitative statistical metrics were used to evaluate the model performance with site observations in different regions (Table 1), including the root-mean-square error (RMSE), mean absolute error (MAE), model coefficient of determination (R^2), and model efficiency (EF). The RMSE and MAE represent the deviation between the observed and simulated values, with smaller values indicating better simulation. The R^2 measures the model's capture of the trend. The EF represents model performance in relation to the observed mean.[106–108] Model performance rating ranges are: $0.25 \leq EF < 0.5$ (satisfactory), $0.5 \leq EF < 0.75$ (good), and $EF \geq 0.75$ (excellent or very good).[109] The specific formulas were calculated as follows:

$$RMSE = \sqrt{\frac{1}{N}\sum_{i=1}^{N}(f_i - y_i)^2} \quad \text{(Equation 5)}$$

$$MAE = \frac{1}{N}\sum_{i=1}^{N}|f_i - y_i| \quad \text{(Equation 6)}$$

$$R^2 = \left(\frac{\sum_{i=1}^{N}(y_i - \overline{y})(f_i - \overline{f})}{\sqrt{\sum_{i=1}^{N}(y_i - \overline{y})^2}\sqrt{\sum_{i=1}^{N}(f_i - \overline{f})^2}}\right)^2 \quad \text{(Equation 7)}$$

$$EF = 1 - \frac{\sum_{i=1}^{N}(f_i - y_i)^2}{\sum_{i=1}^{N}(\overline{y} - y_i)^2} \quad \text{(Equation 8)}$$

where y_i, $\overline{y}$, f_i and $\overline{f}$ are observed CH_4, mean observed CH_4, simulated CH_4, and mean simulated CH_4, respectively, N represents the total number of observations.

Coefficient of variation[102] was introduced to evaluate the discrepancies between different scenarios (Figure 5C):

$$CV = \frac{\sqrt{\frac{1}{N}\sum_{i=1}^{N}(X_i - \overline{X})^2}}{\overline{X}} \times 100\% \quad \text{(Equation 9)}$$

where X_i denotes the CH_4 emissions simulated under each scenario, $\overline{X}$ is the mean value of all the scenarios, and N is the total number of scenarios.

Software programs used for all statistical analysis are shown in key resources table section.